

A Parthenogenesis Gene Candidate and Evidence for Segmental Allopolyploidy in Apomictic *Brachiaria decumbens*

Margaret Worthington,^{*1} Christopher Heffelfinger,[†] Diana Bernal,^{*2} Constanza Quintero,^{*} Yeny Patricia Zapata,^{*} Juan Guillermo Perez,^{*} Jose De Vega,[†] John Miles,^{*} Stephen Dellaporta,[†] and Joe Tohme^{*}

^{*}International Center for Tropical Agriculture (CIAT), Cali 763537, Colombia, [†]Department of Molecular, Cellular, and Developmental Biology, Yale University, New Haven, Connecticut 06520, and [‡]The Genome Analysis Centre, Norwich Research Park, Colney, Norwich NR4 7UH, United Kingdom

ORCID IDs: 0000-0001-8019-165X (M.W.); 0000-0003-2847-5158 (J.D.V.)

ABSTRACT Apomixis, asexual reproduction through seed, enables breeders to identify and faithfully propagate superior heterozygous genotypes by seed without the disadvantages of vegetative propagation or the expense and complexity of hybrid seed production. The availability of new tools such as genotyping by sequencing and bioinformatics pipelines for species lacking reference genomes now makes the construction of dense maps possible in apomictic species, despite complications including polyploidy, multisomic inheritance, self-incompatibility, and high levels of heterozygosity. In this study, we developed saturated linkage maps for the maternal and paternal genomes of an interspecific *Brachiaria ruziziensis* (R. Germ. and C. M. Evrard) × *B. decumbens* Stapf. F₁ mapping population in order to identify markers linked to apomixis. High-resolution molecular karyotyping and comparative genomics with *Setaria italica* (L.) P. Beauv provided conclusive evidence for segmental allopolyploidy in *B. decumbens*, with strong preferential pairing of homologs across the genome and multisomic segregation relatively more common in chromosome 8. The apospory-specific genomic region (ASGR) was mapped to a region of reduced recombination on *B. decumbens* chromosome 5. The *Pennisetum squamulatum* (L.) R.Br. *PsASGR-BABY BOOM-like* (*psASGR-BBML*)-specific primer pair p779/p780 was in perfect linkage with the ASGR in the F₁ mapping population and diagnostic for reproductive mode in a diversity panel of known sexual and apomict *Brachiaria* (Trin.) Griseb. and *P. maximum* Jacq. germplasm accessions and cultivars. These findings indicate that *ASGR-BBML* gene sequences are highly conserved across the Paniceae and add further support for the postulation of the *ASGR-BBML* as candidate genes for the apomictic function of parthenogenesis.

KEYWORDS polyploidy; genetic linkage map; apospory; genotyping by sequencing; molecular karyotyping

APOMIXIS, asexual reproduction through seed, results in progeny that are genetically identical to the female parent (Asker and Jerling 1992). Apomictic reproduction is found naturally in many economically important forage grass

genera and is highly desirable in the sense that superior heterozygous genotypes can be propagated faithfully through seed over many generations without the expense and difficulty of hybrid seed production from inbred parental lines or vegetative propagation. Apospory, a common form of apomixis found in Paniceae grass genera including *Brachiaria* (Trin.) Griseb. (syn. *Urochloa*), *Cenchrus* L./*Pennisetum* Rich., *Panicum* L. (syn. *Megathrysis*), and *Paspalum* L. involves two sequential processes. An unreduced embryo sac first develops from an adjacent somatic nucellar cell (apomeiosis), which then develops into a viable embryo without fertilization (parthenogenesis) (Barcaccia and Albertini 2013; Hand and Koltunow 2014). Recently, the *ASGR-BBML* gene family has been postulated as candidate genes for parthenogenesis

Copyright © 2016 by the Genetics Society of America

doi: 10.1534/genetics.116.190314

Manuscript received April 11, 2016; accepted for publication May 14, 2016; published Early Online May 20, 2016.

Available freely online through the author-supported open access option.

Supplemental material is available online at www.genetics.org/lookup/suppl/doi:10.1534/genetics.116.190314/-/DC1.

¹Corresponding author: International Center for Tropical Agriculture, Tropical Forages, Km 17 Recta Cali-Palmira, Valle del Cauca 763537, Colombia. E-mail: m.worthington@cgiar.org

²Present address: Department of Chemistry and Chemical Biology, Northeastern University, Boston, MA 02115.

in the genus *Cenchrus/Pennisetum* (Conner *et al.* 2015). However, the role of the *ASGR–BBML* has yet to be established in other apomictic species and many questions remain regarding the role of apomixis in genomic stability and polyploid evolution. To date, these questions have largely been addressed through cytogenetic studies (*e.g.*, Mendes-Bonato *et al.* 2002) or population genetics (*e.g.*, Akiyama *et al.* 2011; Lovell *et al.* 2013). The development of dense genetic maps in apomictic species would complement these studies and facilitate molecular breeding in tropical forages, but factors including lack of investment, self-incompatibility, multisomic inheritance, and high levels of heterozygosity have thus far prevented the construction of saturated linkage maps in polyploid apomicts.

Brachiaria forage grasses are widely sown across the global, and especially American tropics, where they have drastically increased the efficiency of cattle production, particularly in areas with marginal soils (Miles *et al.* 2004). *Brachiaria* grasses are most economically important in Brazil, where they are planted on 99 Mha, accounting for 85% of sown pasture land (Jank *et al.* 2014). In addition to extensive pasture systems in Latin America, *Brachiaria* is also planted in intensive smallholder systems in Africa and Asia (Hare *et al.* 2013; Khan *et al.* 2014; Maass *et al.* 2015). The three most important commercial species, *Brachiaria brizantha* (A. Rich.) Stapf (palisadegrass), *B. decumbens* Stapf (signalgrass), and *B. humidicola* (Rendle) Schweick (koronivia-grass) exist primarily as apomicts with varying levels of polyploidy, although diploid sexual genotypes are also found in nature (Valle and Savidan 1996). *B. brizantha* and *B. decumbens* form an agamic complex with a diploid sexual species of lesser commercial importance, *B. ruziziensis* Germain & Evrard (ruzigrass) ($2n = 2x = 18$) (Lutts *et al.* 1991). Microsporogenesis occurs normally in apomictic plants; therefore, apomictic genotypes can be crossed to sexual plants as pollen donors to generate progeny segregating for reproductive mode. Thus, the development of a synthetic autotetraploid sexual ($2n = 4x = 36$) *B. ruziziensis* genotype through colchicine doubling (Swenne *et al.* 1981) facilitated recombination between sexual plants and tetraploid apomictic *Brachiaria* pollen donors and enabled the establishment of breeding programs at the International Center for Tropical Agriculture (CIAT) and Empresa Brasileira de Pesquisa Agropecuária (EMBRAPA) (Brazilian Enterprise for Agricultural Research) in the late 1980s (Miles 2007).

Efficient and reliable discrimination between apomictic and sexual offspring is of paramount importance to *Brachiaria* breeding programs because only apomict genotypes can be released as true-breeding cultivars (Miles 2007). Apospory is usually inherited as a single dominant Mendelian factor denoted as the apospory-specific genomic region (ASGR) (Ozias-Akins and van Dijk 2007). Thus, the progeny generated from a cross between a sexual female parent and an apomictic pollen donor are expected to segregate for reproductive mode on a 1:1 basis. Embryo sac analysis and progeny tests can be used to assess individuals in segregating

populations for reproductive mode, but both are time consuming and expensive. In contrast, molecular markers tightly linked to apomixis can be used to inexpensively and rapidly assess the reproductive mode of thousands of segregating progeny at the seedling stage (Worthington and Miles 2015).

Marker-assisted selection (MAS) for apomixis has been used routinely in the CIAT *Brachiaria* breeding program since 2009, providing considerable savings in time and money used to establish sexual hybrids unsuitable for further use in the breeding program (Worthington and Miles 2015). The marker used to screen new hybrids is a sequenced characterized amplified region (SCAR) marker named “N14” developed from a random amplified polymorphic DNA (RAPD) marker linked to apomixis in *B. decumbens* CIAT 606 (cv. Basilisk) and *B. brizantha* CIAT 26646 (cv. La libertad) (Pedraza Garcia 1995). N14 is diagnostic for apomixis when CIAT 606 is used as the pollen parent, but performs inconsistently in populations derived from crosses with some apomict accessions of *B. decumbens* and *B. brizantha* and does not amplify in the more distantly related commercial species *B. humidicola* (J. Miles, C. Quintero, and J. Tohme, unpublished data). Parallel mapping efforts at EMPRAPA with amplified fragment length polymorphism (AFLP) markers and restriction fragment length polymorphism (RFLP) probes developed in maize and rice showed that apomixis in *B. brizantha* CIAT 6294 (cv. Marundu) was linked to a total of nine markers. Four linked markers were syntenic with maize chromosome 5 and two markers were syntenic with rice chromosome 2, which in turn is also mostly syntenic with maize chromosome 5 (Pessino *et al.* 1997, 1998). Another recent study identified a RAPD marker linked to apomixis in *B. humidicola* (Zorzatto *et al.* 2010). However, CIAT researchers were unable to generate bands linked to apomixis in segregating *B. humidicola* crosses using the published primers.

Apomixis research is relatively more advanced in the related Paniceae genus *Cenchrus/Pennisetum*. In *Pennisetum squamulatum* (L.) R. Br. (syn. *Cenchrus squamulatus*), the ASGR has been mapped to a physically large hemizygous region of reduced recombination (Ozias-Akins *et al.* 1998). Sequence analysis of bacterial artificial chromosome (BAC) clones in *P. squamulatum* revealed the presence of multiple copies of the *PsASGR–BABY BOOM-like* (*PsASGR–BBML*) gene in the ASGR region (Conner *et al.* 2008). The *ASGR–BBML* genes have been posited as candidate genes for parthenogenesis in *Pennisetum* and *Cenchrus* based on multiple lines of evidence, including similarity to *BABY BOOM* (*BBM*) genes associated with somatic embryogenesis in *Brassica* and *Arabidopsis* (Boutillier 2002), failed parthenogenesis in a recombinant *C. ciliaris* plant lacking *CcASGR–BBML* genes (Conner *et al.* 2013), reduced parthenogenic embryo development in apomictic F_1 RNA interference (RNAi) transgenic plants with reduced *PsASGR–BBML* expression (Conner *et al.* 2015), and induced parthenogenesis and production of haploid offspring in transgenic sexual pearl millet plants expressing *PsASGR–BBML* (Conner *et al.* 2015). The primer pair p779/p780 was developed from sequences in the fourth and seventh exons of

ASGR-BBM-like2 and amplifies a region including three introns of 95 bp, 266 bp, and 154 bp (Akiyama *et al.* 2011). This primer pair was linked to the ASGR in F₁ populations developed with *P. squamulatum* and *C. ciliaris* as apomictic pollen parents and validated in a diversity panel of apomictic and sexual *Pennisetum* and *Cenchrus* species, where it amplified in all apomictic species but no sexual species (Akiyama *et al.* 2011). The presence of *ASGR-BBML* genes in other aposporous Paniceae genera and potential of p779/p780 as a diagnostic marker for apomixis in tropical forage grass breeding programs has yet to be tested.

Genetic framework maps have been constructed with AFLP and RFLP markers in several aposporous Paniceae genera including *Cenchrus* (Jessup *et al.* 2003), *Panicum* (Ebina *et al.* 2005), *Paspalum* (Stein *et al.* 2007), and *Brachiaria* (Thaikua *et al.* 2016). However, these maps are generally poorly saturated, with fewer linkage groups than expected for a pseudotestcross map with a separate linkage group for each chromosome or an excess of very sparse and/or short linkage groups. Some efforts have been made to assess homology among linkage groups and assess the prevalence of preferential pairing in polyploid species (Jessup *et al.* 2003; Stein *et al.* 2007). While tetrasomic inheritance was proposed for *Paspalum notatum* Flügge (Stein *et al.* 2007), preferential (disomic) chromosome pairing was also identified in certain chromosomal segments including the apospory linkage group (Stein *et al.* 2004). Jessup *et al.* (2002) also found evidence for disomic inheritance of the apospory linkage group in *C. ciliaris* L. However, the ratio of repulsion- vs. coupling-phase linkages in the maternal and paternal genetic maps suggests that *C. ciliaris* is a segmental allopolyploid with substantial variation in the relative prevalence of multisomic and disomic pairing among parental genotypes (Jessup *et al.* 2003). Evidence regarding ploidy and chromosomal pairing in *Brachiaria* is limited to cytogenetic studies. Bivalent chromosome associations were predominant in a panel of *B. brizantha* accessions and in *B. decumbens* CIAT 606; however, a low frequency of multivalent associations in all tested polyploids suggested that they may be segmental allopolyploids composed of partially homologous subgenomes (Mendes-Bonato 2002; Mendes-Bonato *et al.* 2002).

Recent advances such as genotyping by sequencing (GBS) and bioinformatics pipelines for species lacking reference genomes make the construction of dense maps possible in polyploid apomict species despite their complicated genomics. GBS is a high-throughput genotyping platform that uses a reduced representation library strategy to reduce the genome to a subset of restriction enzyme recognition sites and integrate single nucleotide polymorphism (SNP) discovery and genotype calling into a single step (Elshire *et al.* 2011). GBS has been used to generate saturated genetic maps in highly heterozygous clonally propagated specialty crops with few molecular resources such as red raspberry (*Rubus ideaus* subsp. *ideaus* L.) (Ward *et al.* 2013) and is much more cost effective for developing high-density linkage maps than fixed SNP arrays in specialty crops. This is especially true for multi-

somic polyploids, where only the fraction of markers with simplex segregation patterns can be mapped using a pseudotestcross strategy in software designed for diploid species (Van Ooijen 2011). Recently GBS was also used to construct a saturated genetic linkage map in an autotetraploid alfalfa (*Medicago sativa* L.) F₁ mapping population (Li *et al.* 2014) using a pseudotestcross strategy, demonstrating the effectiveness of this approach in multisomic polyploid species.

The principal objective of this study was to develop the first saturated linkage maps of polyploid apomict species using GBS in an interspecific *B. ruziziensis* × *B. decumbens* ($2n = 4x = 36$) F₁ mapping population ($n = 169$), segregating for reproductive mode. These saturated maps were then used to assess synteny with foxtail millet (*Setaria italica* (L.) P. Beauv), a diploid sexual species in the tribe Paniceae, and evaluate meiotic interactions among homologs and homeologs by molecular karyotyping. Lastly, the genetic mapping population and a diversity panel of *Brachiaria* and *Panicum* accessions with known reproductive mode were used to identify flanking markers linked to the ASGR in *B. decumbens* and test for conservation of *ASGR-BBML* genes across the Paniceae using the primer pair p779/p780.

Materials and Methods

Evaluation of reproductive mode

Parents and F₁ progeny of the BRX 44-02 (*B. ruziziensis*) × CIAT 606 (*B. decumbens*) mapping population were classified as apomictic or sexual by cytoembryological observation of benzyl benzoate:dibutyl phthalate-cleared pistils using differential interference contrast (DIC) microscopy following Crane and Carman (1987) with minor modifications. At least 30 pistils with normally developed embryo sacs were evaluated for each of the 167 F₁ progeny assessed for reproductive mode. Progeny with only Polygonum type embryo sac development were scored as sexual, while progeny with any pistils that had enlarged vacuolated nucellar cells or further Panicum-type embryo sac development were scored as apomictic.

GBS and SNP genotype calling

GBS libraries were prepared following Heffelfinger *et al.* (2014). The methylation-sensitive restriction enzyme *HincII* [R0103; New England Biolabs (NEB)], which recognizes a degenerate six-bp sequence, was used for digestion. Libraries were constructed for the 169 F₁ progenies and the two parents and were sequenced as 75-bp paired-end reads on the Illumina HiSeq 2500 in rapid run mode by the Yale Center for Genome Analysis (<http://medicine.yale.edu/keck/ycga/index.aspx>) following the manufacturer's protocol. Depths of coverage for each sample are provided in Supplemental Material, Table S1. *De novo* SNP discovery and genotype calling was conducted using the Tassel 3.0 Universal Network Enabled Analysis Kit (UNEAK) pipeline (Lu *et al.* 2013). A greater number of reads are required to make accurate genotypic calls in tetrasomic polyploid populations than

diploid populations. Thus, strict genotype calling thresholds were employed following the recommendations of Li *et al.* (2014) in order to reliably distinguish between homozygotes (AAAA) and triplex heterozygotes (AAAB).

PCR-based marker reactions

The parents and progeny of the mapping population were also evaluated with the SCAR marker N14, *ASGR-BBML*-specific primers p779/p780, and six Kompetitive allele-specific PCR (KASP) assays (K42517, K62444, K76831, K100912, K171196, and K207542) designed based on *ASGR*-linked GBS markers from the CIAT 606 parental map (Table S2, Table S3). The four most tightly linked KASP markers, N14, and p779/p780 were also used to evaluate a *Brachiaria* diversity panel composed of *B. brizantha*, *B. decumbens*, *B. ruziziensis*, and *B. humidicola* accessions with a mixture of apomictic, sexual, and unknown reproductive mode from the CIAT genetic resources program forages collection and four interspecific apomictic hybrid cultivars. Five *C. ciliaris* accessions and 10 *P. maximum* accessions with mixed reproductive mode were also evaluated with N14 and p779/p780.

Linkage map construction

Separate genetic linkage maps of BRX 44-02 and CIAT 606 were constructed in JoinMap 4.1 following the two-way pseudotest-cross strategy (Van Ooijen 2011). Markers that were heterozygous in only one parent, had <20% missing data, and had a segregation ratio of heterozygote-to-homozygote progeny of <2:1 were classified as single-dose allele (SDA) markers and used in map construction. Markers that were heterozygous in BRX 44-02 and fit the expected 5:1 segregation ratio for double-dose allele (DDA) markers were used to identify homologs and in the maternal haplotype map and to generate joint linkage maps for *B. ruziziensis* chromosomes 1–9 in TetraploidMap (Hackett *et al.* 2007). Areas of segregation distortion were identified based on deviation of SDA markers from expected allelic ratios according to the χ^2 -test following Li *et al.* (2014).

Syntenic analysis and molecular karyotyping

Extended tag pair sequences of SDA and DDA markers were queried against the foxtail millet genome (<http://www.phytozome.net/foxtailmillet.php>). Markers that aligned to a unique position in the foxtail millet genome ($P < 1e-4$) were used to assign each linkage group to a chromosome and identify homologs. High-resolution molecular karyotyping was then used to detect meiotic associations between chromosomal regions with differing degrees of homology and homeology across the paternal CIAT 606 genome following Mason *et al.* (2014). Chromosome segregation and recombination events in CIAT 606 were also manually inspected by visualization of changes in allele presence or absence along the parental haplotype map in the progeny.

Data availability

File S1 contains a list with detailed information for all the supplemental tables and figures. More detailed informa-

tion about the materials and methods used in this study can be found in File S2. Table S1 provides information on depth of coverage for parents and progeny. KASP primer sequences are given in Table S2. Table S3 contains the genotype scores of p779/p780, N14, KASP assays, and the GBS-derived SDA and DDA markers evaluated in the BRX 44-02 \times CIAT 606 population. UNEAK sequences of the GBS-derived SDA and DDA markers with variant alleles designated as “query” and “hit” according to Lu *et al.* (2013) can be found in Table S4. Breeders and scientists interested in applying p779/p780 in their own programs can access information including primer sequences, PCR conditions, and genetic resources at the Integrated Breeding Program diagnostic marker site (<https://www.integratedbreeding.net/298/breeding-services/predictive-markers?marker=58>).

Results

Analysis of reproductive mode

The 167 F_1 phenotyped progeny segregated for reproductive mode at a 1:1 ratio ($\chi^2 = 0.006$, $P = 0.94$) (Table 1, Table S5), supporting the hypothesis that apospory is inherited as a single dominant genetic factor in *Brachiaria*. A small portion of pistils with abnormal embryo sacs were found in both apomictic and sexual plants (Table S5, Figure S1J). Progeny classified as sexual had only Polygonum-type embryo sacs in all normally developed pistils, while progeny classified as apomictic had normally developed pistils with only Panicum-type embryo sacs, only Polygonum-type embryo sacs, or with Panicum- and Polygonum-type embryo sacs together. The average proportion of Panicum-type embryo sacs observed in progeny classified as apomicts was 0.57 and ranged from 0.07 to 1.00 (Table S5, Figure S2). Apomictic progeny had significantly more embryo sacs per pistil than sexually reproducing progeny ($P < 0.01$). Sexual progeny usually had a single embryo sac per pistil (Table 1, Table S5), although four sexual plants had a low portion of “twin” embryo sac development. In contrast, plants scored as apomicts often had multiple embryo sacs per pistils (Table 1, Table S5, Figure S1, F–I).

GBS

After quality filtering and processing with the UNEAK pipeline, a total of 87.4 million of the original 484.1 million sequencing reads (Table S1) were assigned to 147,496 tag pair sites. After markers with a missing genotype score in either parent were removed, a total of 10,479 polymorphic GBS markers were identified with an average of 44% missing genotype calls per marker in the F_1 progeny. Of these markers, 3912 had <20% missing genotype calls among the F_1 progeny. Within the data set with a maximum threshold of 20% missing data per marker, a total of 1916 markers (49%) were classified as SDAs. Of the SDA markers, 706 markers were heterozygous in BRX 44-02 and 1210

Table 1 Reproductive mode of the F₁ progeny of the BRX 44-02 × CIAT 606 mapping population

Reproductive mode	No. of progeny	Proportion of Polygonum-type embryo sacs	Proportion of Panicum-type embryo sacs	Embryo sacs per pistil
Sexual	84	1	0	1.00
Apomictic	83	0–0.93	0.07–1	2.11
Total	167			

The range of proportion Polygonum- and Panicum-type embryo sacs observed in the progeny of each phenotypic class, and average number of embryo sacs per pistil observed in progeny classified as sexual and apomictic are also shown.

markers were heterozygous in CIAT 606. A further 281 (8%) markers in the data set fit a 5:1 segregation ratio (χ^2 , $P < 0.05$) and were classified as DDAs. Two hundred and sixty-one of the DDA markers were heterozygous in BRX 44-02, while only 20 of the markers were heterozygous in CIAT 606. The ratio of SDA-to-DDA markers in BRX 44-02 was 3:1, while the SDA:DDA ratio was 61:1 in CIAT 606 (Table S6).

Genetic linkage maps and synteny with foxtail millet

The 706 GBS SNP markers heterozygous in BRX 44-02 were placed in 34 linkage groups, with between 3 and 71 markers per linkage group and 2 ungrouped markers (Table 2, Table S7, Figure 1A). The total length of the BRX 44-02 haplotype map was 1985 cM with an average marker density of 1 per 2.8 cM. The 1210 GBS SNP markers heterozygous in CIAT 606 and markers N14 and p779/p780 were assigned to 36 linkage groups in JoinMap 4.1 (Table 2, Table S7, Figure 1B). The number of markers per linkage group ranged from 14 to 72. The total map length was 2693 cM, with an average of 1 marker every 2.2 cM.

Two hundred and twelve (30%) and 356 (29%) of the GBS SNP markers heterozygous in BRX 44-02 and CIAT 606, respectively, mapped to unique positions on the foxtail millet reference genome at a cutoff E -value of $<1 \times 10^{-4}$ (Figure 2, Table S7). However, the distribution of markers with unique positions on the foxtail millet physical map was uneven across chromosomes. The number of markers mapped to each chromosome of foxtail millet ranged from 33 (chromosome 8) to 90 (chromosome 3) (Table S7). Using this information, we were able to identify the four homologous linkage group chromosomes from the CIAT 606 genetic map corresponding to each of the nine base chromosomes of *B. decumbens* and assign them names based on synteny with diploid foxtail millet ($2n = 2x = 18$) (Figure 2B).

The BRX 44-02 maternal genetic map had several poorly saturated linkage groups and only 26 of 34 linkage groups with >2 markers that mapped to unique physical positions in a single foxtail millet chromosome (Figure 2A). Therefore, shared linkages with DDA markers were used to complement synteny data and assist in the identification of homologous linkage groups (Table S8). While most *B. ruziziensis* chromosomes had 4 linkage groups corresponding to each of the four haplotypes (homologous chromosomes), chromosomes 2 and 9 had only 3 corresponding linkage groups (Table 2, Table S7). One of the 2 unlinked markers mapped to a unique physical position

on foxtail millet chromosome 2 and was linked to a DDA marker, which also had shared linkage with SDAs mapped to *B. ruziziensis* linkage groups 2 a–c, indicating that it likely is the lone marker from the fourth homolog of *B. ruziziensis* chromosome 2 (Table S8, Table S9, Figure S3). Combined linkage maps for each *B. ruziziensis* chromosome, generated with 50 markers selected from each homologous linkage group and DDAs in linkage with those SDA haplotypes, ranged in length from 83 to 116 cM (Table S8, Figure S3). Synteny with foxtail millet was conserved in the joint map, indicating that map ordering was correct (Figure S4).

The only observed reciprocal translocation between *Brachiaria* and foxtail millet was between the proximal tip of chromosome 3 (0–2 Mbp) and the distal tip of chromosome 7 (33–36 Mbp) (Table S7, Table S9, Figure S4, Figure S5). Inversions between the foxtail millet physical map and *B. ruziziensis* and *B. decumbens* genetic maps were relatively more common. A consistent inversion was observed between the proximal arm of foxtail millet chromosome 1 and the CIAT 606 haplotype maps (1 a–d) and BRX 44-02 chromosome 1 joint map. Other inversions between the proximal arm of foxtail millet chromosomes 3, 5, and 6 and the BRX 44-02 joint genetic maps of those chromosomes (Table S9, Figure S4) were supported by parallel inversions in at least two of the four CIAT 606 haplotype maps for each chromosome, although the marker density in the remaining haplotype maps was not sufficient to verify whether the inversion was present in all homologs of *B. decumbens* (Table S7, Figure S5).

Preferential pairing

A strong peak in segregating allele read frequency (ratio of reads for the segregating allele to total reads) was observed around 0.25 for GBS SDA markers included in the BRX 44-02 maternal haplotype map, as expected for SDA markers in an autotetraploid parent (AAAB) (Figure 3A). In contrast, two peaks at 0.25 and 0.5 were observed for segregating allele read frequency in GBS SDA markers in the CIAT 606 genetic map (Figure 3B). The peak at 0.5 is stronger than the peak at 0.25, indicating that some SNPs are present in all four haplotypes of each chromosome, but the majority of SNPs are found in only one of two differentiated subgenomes of *B. decumbens*. A third peak in segregating allele read frequency around 0.33 is likely the result of the overlapping tails of the normal curves around peaks at 0.25 and 0.5.

Table 2 Distribution of single-dose allele markers across the 70 linkage groups of the BRX 44-02 and CIAT 606 haplotype maps.

Linkage group	BRX 44-02			CIAT 606		
	No. of markers	Length (cM)	Mean read ratio of heterozygous parent	No. of markers	Length (cM)	Mean read ratio of heterozygous parent
1a	34	90.2	0.34	44	63.7	0.42
1b	28	81.5	0.34	41	77.1	0.47
1c	27	76.6	0.28	32	44.5	0.34
1d	3	55.9	0.33	23	48.0	0.36
2a	41	91.2	0.32	56	91.8	0.44
2b	34	108.3	0.43	43	83.2	0.45
2c	25	88.3	0.43	29	82.5	0.35
2d	—	—	—	18	78.3	0.34
3a	71	86.8	0.34	58	79.2	0.44
3b	22	61.7	0.26	37	87.7	0.46
3c	20	67.2	0.28	27	100.2	0.29
3d	15	43.8	0.30	23	100.4	0.30
4a	41	66.0	0.30	39	64.5	0.45
4b	9	10.1	0.33	23	56.7	0.46
4c	9	72.3	0.32	19	36.8	0.30
4d	4	14.7	0.27	14	47.7	0.33
5a	21	96.3	0.31	45	98.0	0.49
5b	18	47.7	0.34	41	105.0	0.48
5c	14	95.7	0.25	34	67.1	0.32
5d	7	12.7	0.26	26	101.7	0.36
6a	28	56.5	0.60	50	68.9	0.45
6b	18	33.1	0.28	30	64.2	0.47
6c	12	32.2	0.33	26	64.5	0.29
6d	8	28.7	0.27	23	72.9	0.32
7a	25	80.3	0.30	38	63.7	0.48
7b	24	56.1	0.27	22	57.5	0.43
7c	19	86.9	0.57	27	77.5	0.34
7d	8	56.4	0.28	18	82.9	0.28
8a	27	52.7	0.28	39	49.7	0.28
8b	15	38.7	0.30	20	44.4	0.35
8c	5	33.0	0.19	38	69.1	0.38
8d	3	24.5	0.47	30	56.8	0.34
9a	30	34.2	0.32	71	106.7	0.47
9b	22	33.1	0.39	66	96.2	0.46
9c	17	71.8	0.27	23	98.1	0.33
9d	—	—	—	19	105.4	0.30
Total	704	1985.3	0.34	1212	2692.6	0.40

Length and mean ratio of segregating allele reads to total reads in the heterozygous parent in each of the 70 linkage groups are shown.

High-resolution molecular karyotyping was used to test each marker pair for significant linkage and segregation, enabling the identification of two sets of preferentially pairing homologs for each *B. decumbens* chromosome (Figure 4, Table S10). *B. decumbens* haplotypes were named such that “a” and “b” are a set of preferentially pairing homologs and “c” and “d” form the second set of homologs. There is no evidence that the haplotypes named a and b for any given chromosome belong to the same subgenome as haplotypes a and b in the other chromosomes. Visual inspection of allelic inheritance in the 169 F₁ progeny revealed that 90–99% of segregation patterns matched expectations for homologous pairing in all chromosomes except chromosome 8 (Table 3).

Nonhomologous pairing was relatively more common in *B. decumbens* chromosome 8, with the four haplotypes pairing with their primary homologs only 75% of the time (Table 3). In addition to segregation between the primary homolog

pairs, Figure 4C shows significant segregation between linkage groups a and d, as well as between linkage groups b and c in *B. decumbens* chromosome 8. The segregating allele read ratios are all significantly higher ($P < 0.05$) for haplotypes a and b than c and d in every *B. decumbens* chromosome except 8, indicating that more SNPs are present in all four haplotypes and the subgenomes may be less differentiated in chromosome 8 compared to the rest of the genome (Table 2). Progeny with unbalanced gametes (evidenced by the presence of segregating alleles in three or one of the four haplotypes in each chromosome, instead of two of four as expected) were also observed in five out of nine *B. decumbens* chromosomes. The incidence of unbalanced gametes was higher in progeny with lower primary homolog pairing rates, peaking at 7% in chromosome 8 (Table 3).

The higher incidence of multiosomic pairing in *B. decumbens* chromosome 8 is also demonstrated by the distribution of

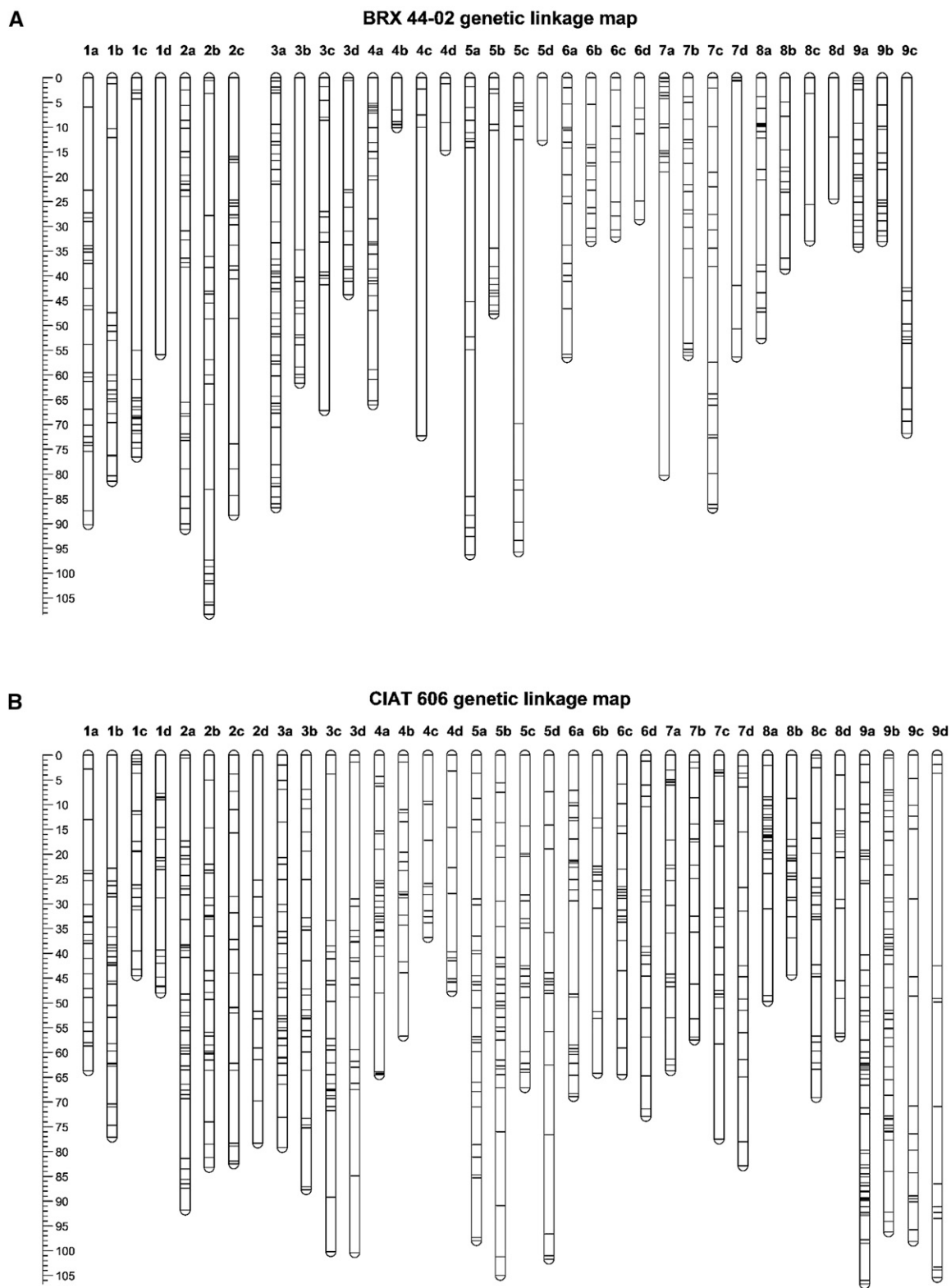


Figure 1 The 34 linkage groups of the BRX 44-02 maternal linkage map (A) and the 36 linkage groups of the CIAT 606 paternal haplotype map (B). Homologous linkage groups a–d were identified and assigned to chromosomes 1–9 based on synteny with foxtail millet (*S. italica*) and shared linkage with DDA markers. Marker position are expressed in centimorgans.

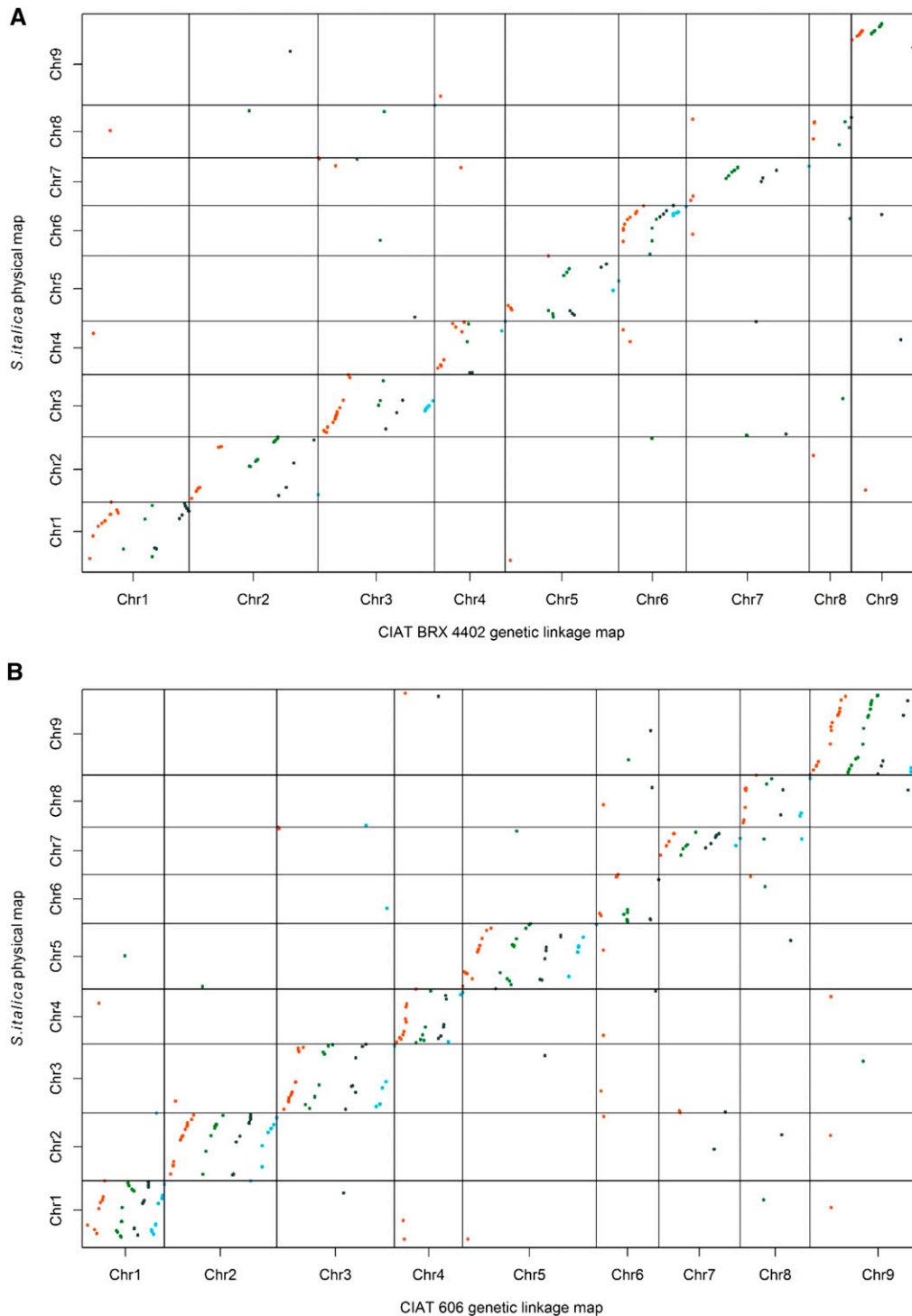


Figure 2 Alignment of markers mapped to the *B. ruziziensis* BRX 44-02 (A) and *B. decumbens* CIAT 606 (B) genetic linkage maps with unique physical positions on the foxtail millet (*S. italica*) reference genome at a cutoff of E -value $< 1 \times 10^{-4}$. Markers mapped to haplotypes a–d of each chromosome are represented with red, blue, green, and violet dots.

DDA markers. Of the 20 GBS markers heterozygous in CIAT 606 that fit the 5:1 segregation ratio of heterozygotes to homozygotes expected for DDAs, 4 were linked in coupling and repulsion with the four haplotypes of chromosome 8 (Table S8). Only 1 other DDA marker was linked to coupling and repulsion with the four haplotypes of chromosome 3. The remaining markers were either in linkage with only two haplotypes from chromosomes 1, 3, 5, 6, or 7 or duplicated in two sets of chromosomes. Interestingly, 7 DDA markers were in

linkage with SDA markers from chromosomes 1 and 4, indicating that these SNPs are duplicated in more than one chromosome.

Segregation distortion

In the BRX 44-02 maternal linkage map, only 21 (3%) of the 704 mapped markers were distorted ($P < 0.01$) (Table S7). No genetic regions met the criteria for distortion (at least 3 distorted markers skewed in the same direction in a region

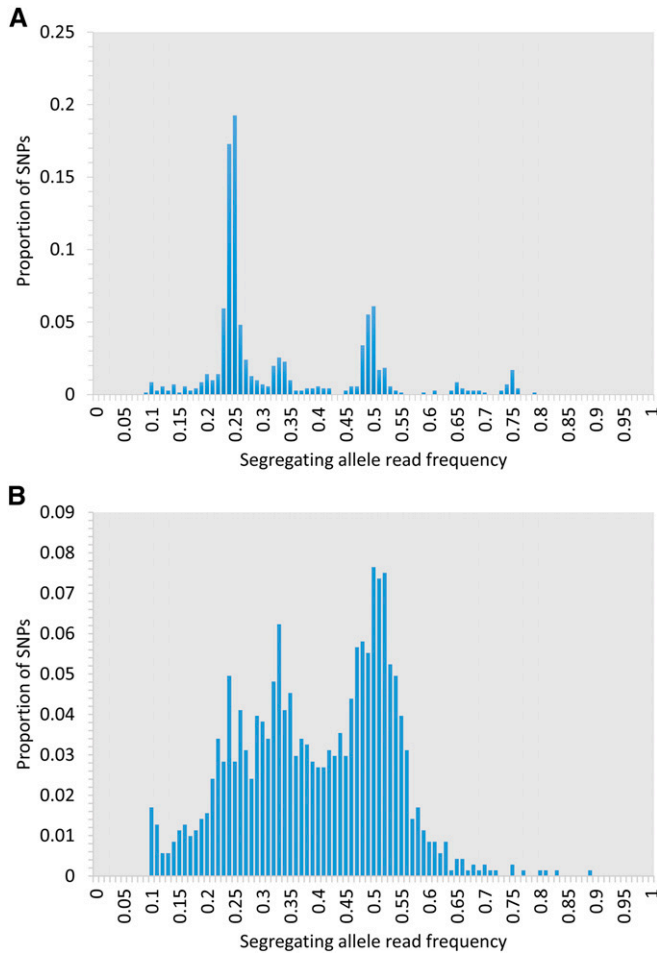


Figure 3 Relative depth of coverage (read frequency) of the segregating allele in heterozygous loci in *B. ruziziensis* BRX 44-02 (A) and *B. decumbens* CIAT 606 (B).

where the smoothed LOESS (locally weighted scatterplot smoothing) curve was over $\text{LOD} = 3.0$ (Figure S6A). However, marker saturation in many maternal haplotypes was poor and regions of segregation distortion could remain undetected. Of the 1212 mapped markers in the CIAT 606 paternal linkage map, 82 (7%) were distorted (Table S7). A major distortion region was identified in haplotypes a and b of CIAT 606 chromosome 9, with an overabundance of heterozygote progeny in the markers mapped to the center of linkage group 9a and an excess of homozygote progeny in the corresponding position of linkage group 9b (Figure S6B).

Genetic mapping of the ASGR

The ASGR was mapped to position 42.5 cM of CIAT 606 linkage group 5c, a region syntenous with foxtail millet chromosome 5 (Table S7, Figure 5). A total of six markers, including the GBS markers TP145804 and TP265637, the GBS-derived KASP markers K42517 and K62444, the SCAR marker N14, and the ASGR–BBML marker p779/p780, were in perfect linkage with the ASGR. The ASGR was flanked at 7.7 cM proximal by TP176128 and at 0.6 cM distal by TP262274,

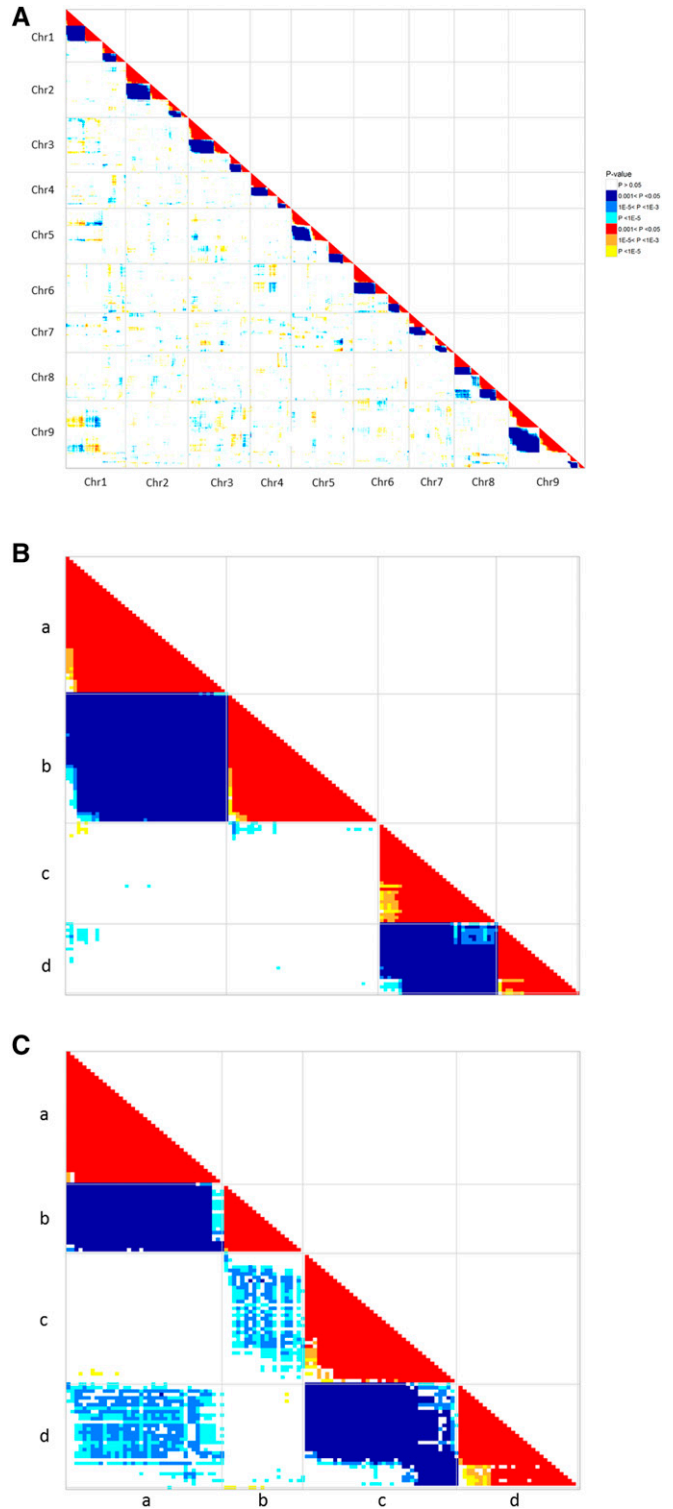


Figure 4 Linkage and segregation of markers in (A) the entire CIAT 606 paternal haplotype map, (B) CIAT 606 chromosome 1 homologs a–d, and (C) CIAT 606 chromosome 8 homologs a–d. SNP markers are arranged by their genetic position (not drawn to scale). Regions with statistically significant linkage are indicated in red, orange, and yellow, while genetic regions with significant segregation are indicated with shades of blue.

Table 3 Percentage of *Brachiaria decumbens* chromosomes segregating with primary homologs

Chromosome	Segregation with primary homolog (%)	Unbalanced gametes ^a (%)
1	95	1
2	95	1
3	96	0
4	90	4
5	96	0
6	95	1
7	98	0
8	75	7
9	99	0
Overall	93	2

These percentages are based on complementary allelic inheritance patterns (presence of segregating alleles in one homolog and absence in the other with or without recombination) between homologs in the 169 F₁ hybrid progeny of the BRX 44-02 × CIAT 606 mapping population and percentage of progeny with unbalanced gametes.

^a Progeny with the segregating alleles present in three or one of the four haplotypes in each chromosome (instead of two of four haplotypes as expected) were classified as unbalanced gametes.

K76831, and K207542. Seventeen of 34 markers mapped to linkage group 5c aligned to unique positions on the foxtail millet chromosome 5 physical map (Table S7, Figure 5). The only marker in perfect linkage with the ASGR that mapped to a unique physical position on foxtail millet chromosome 5 was TP2655637, which aligns to 21.9 Mbp, slightly distal of the centromeric region (Zhang *et al.* 2012). A second marker in perfect linkage with the ASGR, TP145804, mapped to position 41.3 Mbp on foxtail millet chromosome 3, which is also distal to the centromere (Table S7). The distal flanking markers K76831, K207542, and TP262274 map to positions 24.1, 26.4, and 27.8 Mbp on the distal arm of foxtail millet chromosome 5. The proximal arm of *B. decumbens* chromosome 5 is inverted relative to foxtail millet, and the most closely linked proximal marker to the ASGR, which maps to a unique position on the foxtail millet physical map, TP150336, maps to position 5.7 Mbp (Table S7, Figure 5). No markers on the four homologs of *B. decumbens* chromosome 5 were mapped to physical positions in the region 12.5–21.9 Mbp on foxtail millet chromosome 5 (Figure S5).

The ASGR–BBML-specific marker p779/p780, SCAR marker N14, and four KASP markers (K42517, K62444, K76831, and K207542) were subsequently validated in a diversity panel ($n = 162$) comprising four apomictic interspecific *Brachiaria* hybrid cultivars and accessions of *B. brizantha* ($n = 81$), *B. decumbens* ($n = 13$), *B. ruziziensis* ($n = 12$), and *B. humidicola* ($n = 52$) with a mixture of apomictic, sexual, and unknown reproductive mode from the CIAT genetic resources program forages collection. Only p779/p780 was broadly predictive for apomixis in a wide range of *Brachiaria* species and *P. maximum* (Figure 6, Table S11). Markers N14, K42517, K76831, and K207542 all failed to amplify in *B. humidicola*. The KASP marker K62444 amplified well in most *B. humidicola* accessions, but misclassified 30 of 38 accessions with known reproductive mode. In contrast, the primer pair

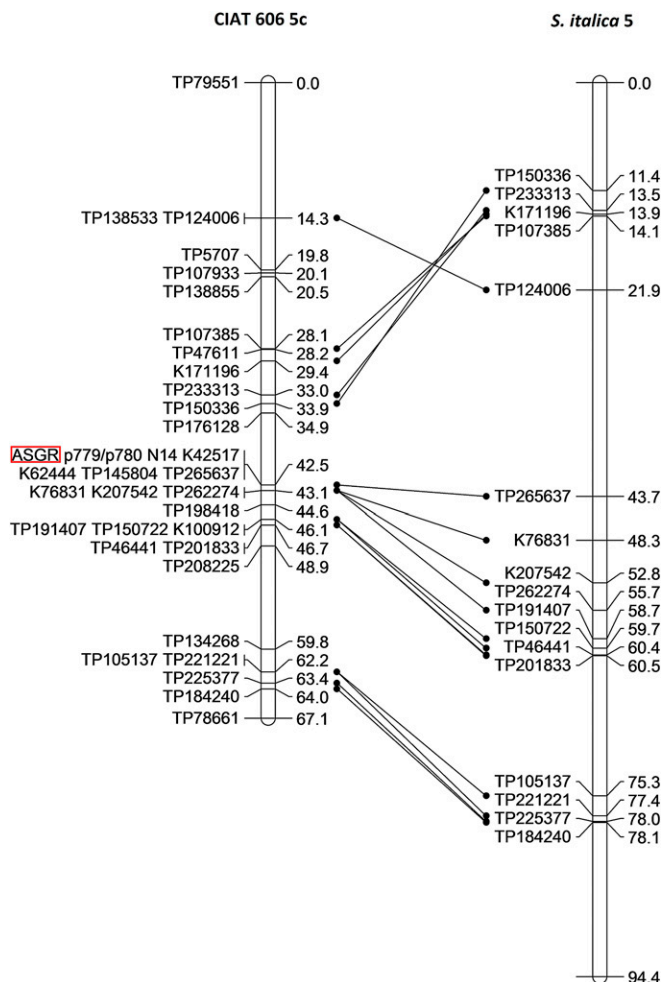


Figure 5 Comparison of CIAT 606 linkage group 5c with the *S. italica* chromosome 5 physical map. Genetic positions are expressed in centimorgans and each unit of the physical map represents 5×10^5 bp. The ASGR is highlighted with a red box

p779/p780 produced bands in all *B. humidicola* samples except CIAT 26146, the only identified natural polyploid sexual accession (Jungmann *et al.* 2010).

N14 and the four KASP markers were better predictors of apomixis in the *B. ruziziensis*/*B. brizantha*/*B. decumbens* agamic complex, but all misclassified at least some accessions with known reproductive mode. Seven, 13, 26, 30, and 31 of the 91 hybrid cultivars and accessions in the *B. ruziziensis*/*B. brizantha*/*B. decumbens* agamic complex classified for reproductive mode were misclassified with N14, K207542, K62444, K76831, and K42517, respectively (Table S11). In comparison *B. decumbens* CIAT 26186 and *B. brizantha* CIAT 26179 were the only apomictic germplasm accessions in the *B. ruziziensis*/*B. brizantha*/*B. decumbens* agamic complex potentially misclassified as sexual by p779/p780. CIAT 26186 was classified as an apomictic tetraploid by EMBRAPA (Penteado *et al.* 2000; Valle *et al.* 2008), but was previously classified as sexually reproducing in unpublished preliminary reproductive mode trials at CIAT. CIAT 26179 was likewise

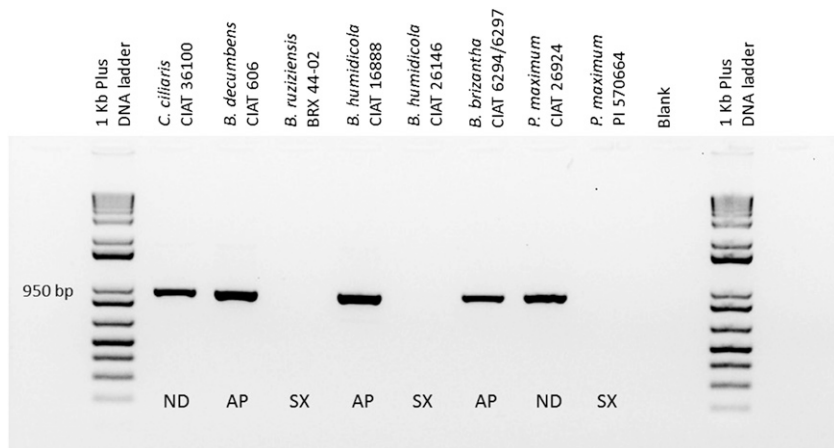


Figure 6 PCR amplification products from the ASGR–BBML primer pair p779/p780 with genomic DNA of *C. ciliaris* 36100, *B. decumbens* CIAT 606, *B. ruziziensis* BRX 44-02, *B. humidicola* CIAT 16888, *B. humidicola* CIAT 26146, *B. brizantha* CIAT 6294/6297, *P. maximum* CIAT 26924, and *P. maximum* PI 570664. Of these materials, BRX 44-02, CIAT 26146, and PI 570664 are putatively sexual. AP, apomictic; SX, sexual; ND, not determined.

classified as an apomictic tetraploid by EMBRAPA (Valle 1990; Penteado *et al.* 2000). This accession has not been phenotyped for reproductive mode at CIAT, but is labeled as a *B. ruziziensis* accession in the CIAT database (<http://isa.ciat.cgiar.org/urg/foragecollection.do>) and fits the taxonomic descriptors for *B. ruziziensis*, a diploid sexual species (Renvoize *et al.* 1996). Thus, research is warranted to determine whether the accessions labeled as CIAT 26186 (EMBRAPA beef cattle (EBC) D017, BRA-004588) and CIAT 26179 (EBC B295) in CIAT and EMBRAPA beef cattle are actually different genotypes. However, the possibility that these are rare ASGR recombinants (Conner *et al.* 2013) cannot be excluded and should be investigated further. The p779/p780 primer pair amplified bands in five *C. ciliaris* accessions and five *P. maximum* accessions from the CIAT genetic resources collection, while failing to produce bands in five putatively sexual progeny of the synthetic autotetraploid Tift sexual *P. maximum* (SPM)92 (US Department of Agriculture plant introduction (PI) 570664) (Figure 6, Table S11). The 10 *C. ciliaris* and *P. maximum* accessions that produced bands when evaluated with p779/p780 were not phenotyped for reproductive mode; however, sexuality is rare in these species.

Discussion

GBS and genetic linkage maps

The higher read depth needed for reliable genotype calling and requirement that only SDA markers be used for mapping in complex tetraploid genomes results in a lower number of total mapped GBS markers compared to diploid, inbred species (Li *et al.* 2014). Still, with 1916 total markers distributed across the parental linkage maps, the maps developed in this study have over three times the marker density of the best currently available genetic maps in tetraploid apomictic species (Jessup *et al.* 2003; Stein *et al.* 2007; Thaikua *et al.* 2016). The total number of sequence reads and average sequence reads per progeny obtained in this study using the GBS protocol of Heffelfinger *et al.* (2014) with the *HincII* restriction enzyme were comparable to those obtained by Li

et al. (2014) in their study of tetraploid alfalfa using the Elshire *et al.* (2011) protocol with ApeKI (R0643L; NEB). Over twice as many polymorphic SNPs were identified in that study; however, the mean percentage of missing genotype calls was much lower in this study and a very similar total number of polymorphic markers with <20% missing data were obtained in the two studies. Overall, both protocols work well and demonstrate the utility of GBS as an approach for the generation of dense genetic maps in complex polyploid species.

Synteny was highly conserved between *B. decumbens*, *B. ruziziensis*, and foxtail millet (*S. italica*), the closest relative of *Brachiaria* with a publicly available reference genome (Zhang *et al.* 2012). The conservation of marker order and genome structure compared to the foxtail millet physical map provided evidence for the validity of the genetic maps and enabled us to assign linkage groups to chromosomes and identify homologs. The only major structural rearrangements identified between *Brachiaria* and foxtail millet were a reciprocal translocation between the proximal and distal tips of chromosomes 3 and 7, and inversions on chromosomes 1, 3, 5, and 6. This marked conservation of genome structure indicates that breeders and geneticists working on *Brachiaria* and other forage genera in the Paniceae would likely benefit from applying the wealth of genomic tools being developed in foxtail millet (Muthamilarasan and Prasad 2015) to their own species.

While the CIAT 606 paternal linkage map had 36 linkage groups, as expected for a tetraploid with a base chromosome number of nine, the BRX 44-02 map had only 34 linkage groups. The lower marker density in the BRX 44-02 maternal haplotype map is not surprising given the synthetic autotetraploid origin of this accession and the high proportion of heterozygous markers fitting DDA segregation ratios. The incorporation of DDA markers with SDA markers from homologous haplotype groups into joint linkage groups resolved some questions about the relative positions of the markers on the individual SDA linkage groups (Hackett *et al.* 2007). However, the utility of this approach would be greatly increased by the development of advanced mapping software

for autopolyploids capable of ordering >50 markers per linkage group.

Preferential pairing and segmental allopolyploidy

The concept of segmental allopolyploidy was first introduced by Stebbins (1947, 1950) as an intermediate form of polyploidy between allopolyploidy and autopolyploidy, where plants composed of partially homologous parental genomes (AAA'A') display a mixture of disomic and multisomic inheritance. Preferential pairing among homologous chromosomes is expected to predominate, with occasional homeologous pairing through the formation of multivalents and/or bivalents with switched pairing partners (A with A'). Segmental allopolyploidy is generally considered a transient state in the evolutionary trajectory of new polyploids toward diploidization and stable allopolyploidy, with exclusive bivalent pairing of primary homologs, or autopolyploidy, with sets of fully homologous chromosomes pairing at random (Sybenga 1996). Previous cytological evidence for segmental allopolyploidy in apomictic *Brachiaria* species was supported by high-resolution molecular karyotyping. Strong preferential pairing among primary homologs was demonstrated by highly significant segregation among alleles mapped to two pairs of homologous SDA linkage groups in each *B. decumbens* chromosome. The presence of two overlapping peaks at 0.25 and 0.5 for segregating allele read frequency in GBS–SDA from the paternal genetic linkage map and the scarcity of markers heterozygous in CIAT 606 that fit the expected segregation ratio for DDAs (5:1) provide secondary supporting evidence for the presence of two related but differentiated subgenomes tetraploid *B. decumbens*.

Successful homologous chromosome pairing and normal bivalent formation in meiosis are highly dependent on sequence similarity. Therefore, meiotic instability and resulting defects, including unbalanced gametes and aneuploidy, are common in F₁ plants derived from wide hybridization events. These problems can generally be resolved by meiotic restitution upon polyploidization through meiotic nonreduction as summarized by De Storme and Mason (2014). However, aneuploid gametes can still be produced by allopolyploid meiosis if nonhomologous pairing and intergenomic recombination compromise the meiotic stability of the parental chromosomal complements (Comai 2005). Therefore, genetic mechanisms such as the *pairing homeologous 1* locus in hexaploid wheat (Sears 1976; Prieto *et al.* 2004) have evolved to prevent homeologous pairing in wheat and promote strict disomic inheritance.

Alternatively, Stebbins (1950) proposed that segmental allopolyploids may stabilize by functional autopolyploidization over many successive generations of recombination between homeologous chromosomes. Stebbins also proposed that a stable (secondary) segmental allopolyploid might evolve with some sets of fully homologous chromosomes and other chromosome sets further differentiated with exclusively preferential pairing, although Sybenga (1996) argued

that no polyploids of this type have been found in nature and segmental allopolyploidy does not occur in established natural polyploids. The evidence for segmental allopolyploidy in *B. decumbens* presented in this study adds to a growing body of literature refuting this claim and demonstrating the existence of naturally occurring segmental allopolyploids in apomict grasses (Mendes-Bonato *et al.* 2002; Jessup *et al.* 2003) and sexually reproducing species (Boff and Schifino-Wittmann 2003; Shinohara *et al.* 2010). The prevalence of segmental allopolyploidy in apomictic grass species suggests that apomixis may effectively arrest the processes of diploidization and/or functional autopolyploidization, enabling genotypes to remain in a neopolyploid state indefinitely.

Additionally, the high-resolution molecular karyotyping approach (Mason *et al.* 2014) used in this study enabled us to evaluate the prevalence of preferential pairing at each individual chromosome. Visual inspection of allelic inheritance in the F₁ progeny indicated that homologs paired preferentially in at least 90% of instances across the genome except in chromosome 8, where significant segregation among markers mapped to secondary homeologs was observed, and segregation patterns in the mapping population progeny suggest that nonhomologous pairing occurs in ~25% of meiotic episodes. Thus *B. decumbens* is the best example to date of a stable (secondary) segmental allopolyploid with most chromosome sets exhibiting strong preferential pairing and chromosome 8 evolving toward functional autopolyploidization.

The presence of meiotic abnormalities is common in both neopolyploids and in the microsporocytes of polyploid apomicts (De Storme and Mason 2014). The most commonly observed meiotic abnormalities observed in polyploid *Brachiaria* were related to irregular chromosome segregation (e.g., precocious migration of univalent to poles in metaphases, laggard chromosomes during anaphases, and formation of micronuclei in microspores), chromosome stickiness, and impaired cytokinesis (Mendes-Bonato *et al.* 2001; Riso-Pascotto *et al.* 2006; Ricci *et al.* 2011a,b). In this study, we also found evidence of progeny with unbalanced gametes in five of nine *B. decumbens* chromosomes, peaking at 7% in chromosome 8. The correlation between nonhomologous pairing and formation of unbalanced gametes observed in this study suggests that apomicts with strong preferential pairing across the genome may produce more viable male gametes. Reduced fertility is considered an important constraint to the success of newly formed polyploids (Ramsey and Schemske 2002). Thus, apomixis may have evolved in unstable segmental allopolyploid grasses as a means to promote fertility despite irregular chromosome segregation caused by nonhomologous pairing in meiosis.

Implications for seed yield and producibility

Although polyploid apomicts are able to forego meiosis during megasporogenesis, the high prevalence of unreduced gamete formation observed in these species is not without consequence for commercial tropical forage seed production. Apomicts in the Paniceae are pseudogamic (Barcaccia and

Albertini 2013), meaning that the secondary nuclei of apomictic embryo sacs must be fertilized with viable pollen gametes for normal endosperm development and seed production. Seed yield potential is an important trait that determines whether a new variety can be profitably produced and distributed to farmers, and failed seed set is a persistent limitation in *Brachiaria*, where caryopsis formation rarely exceeds 30% (Hopkinson *et al.* 1996). Abnormal tetrad frequency appears to be significantly correlated with nonviability of pollen grains (Souza *et al.* 2015). The implications of the relationship between the incidence of meiotic abnormalities and reduced pollen viability are particularly troubling for bred hybrid genotypes. Because there are no known natural allotetraploid sexuals in the *B. ruziziensis*/*B. brizantha*/*B. decumbens* agamic complex, synthetic autotetraploid genotypes (AAAA) have been used as the source of sexuality in inter- and intraspecific crosses with segmental allopolyploid (BBB'B') pollen donors (Swenne *et al.* 1981; Simioni and Valle 2011; Souza *et al.* 2015). Therefore, pairing affinity is likely reduced in progeny (AABB'), which receive male gametes with low homology (BB'). Indeed, meiotic abnormalities appear to be more common in progeny of both inter- and intraspecific crosses than natural apomictic accessions (Risso-Pascotto *et al.* 2005; Fuzinato *et al.* 2007, 2012; Mendes-Bonato *et al.* 2007; Felismino *et al.* 2010; Souza *et al.* 2015). Many natural apomictic accessions, including CIAT 606 (cv. Basilisk), produce adequate seed and are successful as cultivars despite low pollen fertility (Mendes-Bonato *et al.* 2001). Thus, the production of viable pollen may not be as critical in apomictic species as in sexual species, where seed development is dependent on successful pollination of both the embryo and the endosperm (Souza *et al.* 2015). Still, at least one hybrid *Brachiaria* cultivar with excellent forage traits, good stress resistance, and ample flowering failed in the marketplace due to poor seed yield caused by low seed set (Hare *et al.* 2007), indicating that further research on the relationship between meiotic abnormalities and seed yield in tropical forages is warranted.

Inheritance of apomixis and conservation of the ASGR in the Paniceae

Apomixis was inherited as a single dominant Mendelian factor in the BRX 44-02 × CIAT 606 mapping population. Segregation distortion has been associated with apomixis in other apomictic polyploids including *P. notatum* (Martínez *et al.* 2001), *Tripsacum dactyloides* (Grimanelli *et al.* 1998), and interspecific *P. glaucum* × *P. squamulatum* hybrids (Roche *et al.* 2001). However, the only distorted region identified in the present study was on linkage groups a and b on *B. decumbens* chromosome 9, indicating that there may be a lethal or sublethal detrimental factor located on CIAT 606 linkage group 9b.

The ASGR was mapped to position 42.5 cM of CIAT 606 linkage group 5c, a region syntenous with foxtail millet chromosome 5. The number of markers in perfect linkage with the ASGR, large physical distance between ASGR-flanking markers in tight genetic linkage, and proximity of linked

markers to the foxtail millet chromosome 5 centromere all indicate that the ASGR is located in a region of suppressed recombination, as has been demonstrated in *P. squamulatum* (Ozias-Akins *et al.* 1998). Tight clustering of markers in perfect linkage with the ASGR has also been observed in other Paniceae mapping populations (Jessup *et al.* 2002; Martínez *et al.* 2003; Ebina *et al.* 2005; Stein *et al.* 2007; Thaikua *et al.* 2016), although the lack of available information about physical distances between markers in previous studies made it difficult to assess whether recombination was indeed suppressed.

Interestingly, the ASGR was previously linked, in *B. brizantha* CIAT 6294, to RFLP probes designed from rice chromosome 2 and maize chromosome 5 (Pessino *et al.* 1997, 1998). Foxtail millet chromosome 5, on the other hand, is mostly syntenic with rice chromosome 1 and maize chromosome 3 (Zhang *et al.* 2012). The ASGR has also been linked to markers from sorghum chromosome 4, which has homology to maize chromosomes 2 and 10, in *C. ciliaris* (Jessup *et al.* 2002), and rice chromosome 12 in *Paspalum* (Pupilli *et al.* 2004). Most recently, the ASGR-carrier chromosome of *P. squamulatum* was found to be collinear with foxtail millet chromosome 2 and sorghum chromosome 2 by *in silico* transcript mapping and fluorescence *in situ* hybridization (FISH) (Sapkota *et al.* 2016).

Jessup *et al.* (2002) suggested that the implication of different ASGR-carrier chromosomes in these studies may indicate the independent evolution of apomixis in multiple grass species. However, subsequent comparative genomics with ASGR-linked BACs in *Cenchrus* and *Pennisetum* species showed that apomixis more likely evolved as a single event and was spread to other species through hybridization or phylogenetic diversification (Ozias-Akins *et al.* 2003; Akiyama *et al.* 2011). The perfect linkage of the ASGR–*BBML*-specific primers p779/p780 with the ASGR in this mapping population and its excellent diagnostic ability for reproductive mode in the diversity panel indicates conservation of the ASGR in *Cenchrus*/*Pennisetum* and the more distantly related genera *Brachiaria* and *Panicum*. These findings also support the hypothesis of a common origin for aposporous apomixis in the Paniceae tribe. While the ASGR appears to be highly conserved across the Paniceae, the ASGR-carrier chromosome has undergone significant rearrangement and translocation during hybridization. In all apomictic *Pennisetum* species the ASGR is located in the telomeric region of the carrier chromosome, while it is inverted and located in an interstitial region in *Cenchrus* (Goel *et al.* 2006). In *B. decumbens* the ASGR is located adjacent to the centromere of chromosome 5, although previously identified linkages of the *B. brizantha* ASGR with markers from maize chromosome 5 and the lack of transferability of SNPs linked to apomixis in the *B. ruziziensis*/*B. brizantha*/*B. decumbens* agamic complex to *B. humidicola* indicate that the ASGR may have been translocated to different chromosomal backgrounds even within *Brachiaria*.

Conclusions

The development of dense molecular maps in tetraploid *Brachiaria* species has provided useful new information about the genomic organization and evolution of polyploid apomicts. The diagnostic ability of the primers p779/p780 for reproductive mode in the F₁ mapping population and diversity panel of known sexual and apomict *Brachiaria* germplasm accessions and cultivars indicates that *ASGR-BBML* gene sequences are strongly conserved across the Paniceae and adds further support for the postulation of the *ASGR-BBML* as candidate genes for the apomictic function of parthenogenesis. Molecular karyotyping also provided conclusive evidence for segmental allopolyploidy in *B. decumbens*, suggesting that apomixis may have evolved as a means of meiotic restitution to “fix” inherently unstable states of segmental allopolyploidy that would otherwise be lost to natural selection. Future studies focused on comparative genomics of *ASGR* sequences from diverse Paniceae genera should yield interesting information about the evolution of apomixis and may aid in the identification or validation of candidate genes related to aposporous initial formation.

In addition to providing new evidence about the evolution of apospory in the Paniceae and its role in segmental allopolyploidy, the development of saturated genetic linkage maps in polyploid apomict species has immediate applications for tropical forage breeding. The high-density linkage maps developed in this study can be used to map QTL for agronomically important traits in *Brachiaria*, including traits related to pollen fertility and seed yield, and should permit anchoring of sequence scaffolds in the *B. ruziziensis* diploid reference genome. Furthermore, the perfect linkage of p779/p780 with the *ASGR* in the BRX 44-02 × CIAT 606 F₁ mapping population and its excellent predictive ability for reproductive mode in a large diversity panel with multiple species of *Brachiaria* suggest that this is a useful genetic marker for apomixis that can be applied for marker-assisted selection in a wide range of breeding programs. Further research should be conducted to confirm whether p779/p780 is diagnostic for apomixis in populations of *B. humidicola* and *P. maximum* segregating for reproductive mode.

Acknowledgments

We thank CIAT staff whom maintained the population and assisted with the collection of inflorescences for embryo sac analysis including Gerardo Gallego, Aristipo Betancourt, Carlos Dorado, and Gonzalo Rios, as well as staff who participated in the development of previous unpublished AFLP linkage maps in this population including Harold Suarez, Jaime Vargas, Pedro Rocha, and Maryam Chaib de Mares, and Fabio Pedraza-Garcia for his work on the development of N14. Special thanks to Sarah Dyer of The Genome Analysis Center (TGAC) for her collaboration in preparation of the draft *B. ruziziensis* assembly and to John Carman at Utah State University and Robin Hopkins at the Arnold Arboretum for the use of their facilities for embryo

sac analysis. We also thank Alba Lucia Chavez, Maria Eugenia Recio, Narda Jimena Triviño Silva, and Manabu Ishitani for providing DNA for the *Brachiaria* diversity panel. Peggy Ozias-Akins and Joanna Conner at the University of Georgia provided invaluable advice and information on primers p779/p780. Sequencing was performed at the Yale Center for Genome Analysis and computational analyses were performed on the Yale University Biomedical High Performance Computing Cluster, which is supported by NIH grants RR-19895 and RR-029676-01. This work was supported by the Livestock and Fish CGIAR research program.

Author contributions: M.W. provided overall conceptual guidance for the project, conducted molecular mapping, analyzed and interpreted the data, and drafted the manuscript; C.H. conducted bioinformatics and synteny analyses; D.B. phenotyped the mapping population and assisted in manuscript preparation; C.Q. and Y.P.Z. performed library preparation, conducted molecular marker analyses, and assisted in analysis and interpretation of data; J.G.P. assisted in molecular karyotyping analysis and figure preparation; J.D.V. performed the draft assembly of the *B. ruziziensis* diploid genome; J.M. developed the mapping population; and S.D. and J.T. provided conceptual support for the project.

Literature Cited

- Akiyama, Y., and S. Goel, J. A. Conner, W. W. Hanna, H. Yamada-Akiyama *et al.*, 2011 Evolution of the apomixis transmitting chromosome in Pennisetum. *BMC Evol. Biol.* 11: 289.
- Asker, S. E., and L. Jerling, 1992 *Apomixis in Plants*. CRC Press, Boca Raton, FL.
- Barcaccia, G., and E. Albertini, 2013 Apomixis in plant reproduction: a novel perspective on an old dilemma. *Plant Reprod.* 26: 159–179.
- Boff, T., and M. T. Schifino-Wittmann, 2003 Segmental allopolyploidy and paleopolyploidy in species of *Leucaena* benth: evidence from meiotic behaviour analysis. *Hereditas* 138: 27–35.
- Boutillier, K., 2002 Ectopic expression of BABY BOOM triggers a conversion from vegetative to embryonic growth. *Plant Cell Online* 14: 1737–1749.
- Comai, L., 2005 The advantages and disadvantages of being polyploid. *Nat. Rev. Genet.* 6: 836–846.
- Conner, J. A., S. Goel, G. Gunawan, M.-M. Cordonnier-Pratt, V. E. Johnson *et al.*, 2008 Sequence analysis of bacterial artificial chromosome clones from the apospory-specific genomic region of Pennisetum and Cenchrus. *Plant Physiol.* 147: 1396–1411.
- Conner, J. A., G. Gunawan, and P. Ozias-Akins, 2013 Recombination within the apospory specific genomic region leads to the uncoupling of apomixis components in Cenchrus ciliaris. *Planta* 238: 51–63.
- Conner, J. A., M. Mookkan, H. Huo, K. Chae, and P. Ozias-Akins, 2015 A parthenogenesis gene of apomict origin elicits embryo formation from unfertilized eggs in a sexual plant. *Proc. Natl. Acad. Sci. USA* 112: 11205–11210.
- Crane, C. F., and J. G. Carman, 1987 Mechanisms of apomixis in *Elymus rectisetus* from Eastern Australia and New Zealand. *Am. J. Bot.* 74: 477.
- De Storme, N., and A. Mason, 2014 Plant speciation through chromosome instability and ploidy change: cellular mechanisms, molecular factors and evolutionary relevance. *Curr. Plant Biol.* 1: 10–33.

- Ebina, M., H. Nakagawa, T. Yamamoto, H. Araya, S. Tsuruta *et al.*, 2005 Co-segregation of AFLP and RAPD markers to apospory in Guinea grass (*Panicum maximum* Jacq.). *Grassl. Sci.* 51: 71–78.
- Elshire, R. J., J. C. Glaubitz, Q. Sun, J. A. Poland, K. Kawamoto *et al.*, 2011 A robust, simple genotyping-by-sequencing (GBS) approach for high diversity species. *PLoS One* 6: 1–10.
- Felismino, M. F., M. S. Pagliarini, and C. B. Do Valle, 2010 Meiotic behavior of interspecific hybrids between artificially tetraploidized sexual *Brachiaria ruziziensis* and tetraploid apomictic *B. brizantha* (Poaceae). *Sci. Agric.* 67: 191–197.
- Fuzinato, V., M. Pagliarini, and C. Valle, 2012 Meiotic behavior in apomictic *Brachiaria ruziziensis* × *B. brizantha* (Poaceae) progenies. *Sci. Agric.* 69: 380–385.
- Fuzinato, V. A., M. S. Pagliarini, and C. B. Valle, 2007 Microsporogenesis in sexual *Brachiaria* hybrids (Poaceae). *Genet. Mol. Res.* 6: 1107–1117.
- Goel, S., Z. Chen, Y. Akiyama, J. A. Conner, M. Basu *et al.*, 2006 Comparative physical mapping of the apospory-specific genomic region in two apomictic grasses: *Pennisetum squamulatum* and *Cenchrus ciliaris*. *Genetics* 173: 389–400.
- Grimanelli, D., O. Leblanc, E. Espinosa, E. Perotti, D. González de León *et al.*, 1998 Non-Mendelian transmission of apomixis in maize-Tripsacum hybrids caused by a transmission ratio distortion. *Heredity* (Edinb) 80(Pt 1): 40–47.
- Hackett, C. A., I. Milne, J. E. Bradshaw, and Z. Luo, 2007 TetraploidMap for Windows: linkage map construction and QTL mapping in autotetraploid species. *J. Hered.* 98: 727–729.
- Hand, M. L., and A. M. G. Koltunow, 2014 The genetic control of apomixis: asexual seed formation. *Genetics* 197: 441–450.
- Hare, M. D., S. Phengphet, T. Songsiri, N. Sutin, E. S. F. Vernon *et al.*, 2013 Impact of tropical forage seed development in villages in Thailand and Laos: Research to village farmer production to seed export. *Trop. Grassl.* 1: 207–212.
- Hare, M. D., P. Tatsapong, and K. Saiprasert, 2007 Seed production of two *brachiaria* hybrid cultivars in north-east Thailand. 1. Method and time of planting. *Trop. Grassl.* 41: 26–34.
- Heffelfinger, C., C. A. Fragoso, M. A. Moreno, J. D. Overton, J. P. Mottinger *et al.*, 2014 Flexible and scalable genotyping-by-sequencing strategies for population studies. *BMC Genomics* 15: 979.
- Hopkinson, J., F. Souza, S. Diulgheroff, A. Ortiz, and M. Sanchez, 1996 Reproductive physiology, seed production, and seed quality of *Brachiaria*, pp. 125–140 in *Brachiaria: Biology, Agronomy, and Improvement*, edited by J. W. Miles, B. L. Maass, and C. B. Valle. CIAT and EMBRAPA, Palmira, Colombia.
- Jank, L., S. C. Barrios, C. B. Valle, R. M. Simeao, and G. F. Alves, 2014 The value of improved pastures to Brazilian beef production. *Crop Pasture Sci.* 65: 1132–1137.
- Jessup, R. W., B. L. Burson, G. B. Burrow, Y. W. Wang, C. Chang *et al.*, 2002 Disomic inheritance, suppressed recombination, and allelic interactions govern apospory in buffelgrass as revealed by genome mapping. *Crop Sci.* 42: 1688–1694.
- Jessup, R. W., B. L. Burson, G. B. Burrow, Y. W. Wang, C. Chang *et al.*, 2003 Segmental allotetraploidy and allelic interactions in buffelgrass (*Pennisetum ciliare* (L.) Link syn. *Cenchrus ciliaris* L.) as revealed by genome mapping. *Genome* 46: 304–313.
- Jungmann, L., B. B. Z. Vigna, and K. R. Boldrini, A. C. B. Sousa, C. B. Valle *et al.*, 2010 Genetic diversity and population structure analysis of the tropical pasture grass *Brachiaria humidicola* based on microsatellites, cytogenetics, morphological traits, and geographical origin. *Genome* 53: 698–709.
- Khan, Z. R., C. A. O. Midega, J. O. Pittchar, A. W. Murage, M. A. Birkett *et al.*, 2014 Achieving food security for one million sub-Saharan African poor through push-pull innovation by 2020. *Philos. Trans. R. Soc. B Biol. Sci.* 369: 20120284.
- Li, X., Y. Wei, A. Acharya, Q. Jiang, J. Kang *et al.*, 2014 A saturated genetic linkage map of autotetraploid alfalfa (*Medicago sativa* L.) developed using genotyping-by-sequencing is highly syntenous with the *Medicago truncatula* genome. *G3* (Bethesda) 4: 1971–1979.
- Lovell, J. T., O. M. Aliyu, M. Mau, M. E. Schranz, M. Koch *et al.*, 2013 On the origin and evolution of apomixis in *Boechera*. *Plant Reprod.* 26: 309–315.
- Lu, F., A. E. Lipka, J. Glaubitz, R. Elshire, J. H. Cherney *et al.*, 2013 Switchgrass genomic diversity, ploidy, and evolution: novel insights from a network-based SNP discovery protocol. *PLoS Genet.* 9: e1003215.
- Lutts, S., J. Ndikumana, and B. P. Louant, 1991 Fertility of *Brachiaria-Ruziziensis* in interspecific crosses with *Brachiaria-Decumbens* and *Brachiaria-Brizantha*: meiotic behavior, pollen viability and seed set. *Euphytica* 57: 267–274.
- Maass, B. L., C. A. O. Midega, M. Mutimura, V. B. Rahetlah, P. Salgado *et al.*, 2015 Homecoming of *Brachiaria*: improved hybrids prove useful for African animal agriculture. *J. KALRO* 8325: 27–30.
- Martínez, E. J., M. H. Urbani, C. L. Quarin, and J. P. A. Ortiz, 2001 Inheritance of Apospory in Bahiagrass, *Paspalum Notatum*. *Hereditas* 135: 19–25.
- Martínez, E. J., H. E. Hopp, J. Stein, J. P. A. Ortiz, and C. L. Quarin, 2003 Genetic characterization of apospory in tetraploid *Paspalum notatum* based on the identification of linked molecular markers. *Mol. Breed.* 12: 319–327.
- Mason, A. S., J. Batley, P. E. Bayer, A. Hayward, W. A. Cowling *et al.*, 2014 High-resolution molecular karyotyping uncovers pairing between ancestrally related *Brassica* chromosomes. *New Phytol.* 202: 964–974.
- Mendes-Bonato, A., 2002 Unusual cytological patterns of microsporogenesis in *Brachiaria decumbens*: abnormalities in spindle and defective cytokinesis causing precocious cellularization. *Cell Biol. Int.* 26: 641–646.
- Mendes-Bonato, A. B., M. S. Pagliarini, N. Silva, and C. B. Valle, 2001 Meiotic instability in invader plants of signal grass *Brachiaria decumbens* Stapf (Gramineae). *Acta Scientiarum* 23: 619–625.
- Mendes-Bonato, A. B., M. S. Pagliarini, F. Forli, C. B. Valle, and M. I. O. Penteado, 2002 Chromosome numbers and microsporogenesis in *Brachiaria brizantha* (Gramineae). *Euphytica* 125: 419–425.
- Mendes-Bonato, A. B., M. S. Pagliarini, and C. B. Valle, 2007 Meiotic arrest compromises pollen fertility in an interspecific hybrid between *Brachiaria ruziziensis* × *Brachiaria decumbens* (Poaceae: Paniceae). *Braz. Arch. Biol. Technol.* 50: 831–837.
- Miles, J. W., 2007 Apomixis for cultivar development in tropical forage grasses. *Crop Sci.* S-239: 47.
- Miles, J. W., C. B. Valle, I. M. Rao, and V. P. B. Euclides, 2004 *Brachiariagrasses*, pp. 745–783 in *Warm-Season (C4) Grasses*. Agronomy Monograph 45, edited by L. E. Moser, B. L. Burson, and L. E. Sollenberger. American Society of Agronomy, Crop Science Society of America, Soil Science Society of America. Madison, WI.
- Muthamilarasan, M., and M. Prasad, 2015 Advances in *Setaria* genomics for genetic improvement of cereals and bioenergy grasses. *Theor. Appl. Genet.* 128: 1–14.
- Ozias-Akins, P., Y. Akiyama, and W. W. Hanna, 2003 Molecular characterization of the genomic region linked with apomixis in *Pennisetum/Cenchrus*. *Funct. Integr. Genomics* 3: 94–104.
- Ozias-Akins, P., and P. J. van Dijk, 2007 Mendelian genetics of apomixis in plants. *Annu. Rev. Genet.* 41: 509–537.
- Ozias-Akins, P., D. Roche, and W. W. Hanna, 1998 Tight clustering and hemizygoty of apomixis-linked molecular markers in *Pennisetum squamulatum* implies genetic control of apospory

- by a divergent locus that may have no allelic form in sexual genotypes. *Proc. Natl. Acad. Sci. USA* 95: 5127–5132.
- Pedraza Garcia, F. P., 1995 Hacia la localización del gen de apomixis en *Brachiaria* usando marcadores moleculares RAPD. Ph. D. thesis, Universidad Nacional de Colombia, Palmira, Valle del Cauca.
- Penteado, M. I. D. O., A. C. M. dos Santos, I. F. Rodrigues, C. B. Valle, M. A. C. Seixas *et al.*, 2000 *Determinacao de ploidia e avaliacao da quantidade de DNA total em diferentes especies do genero Brachiaria*, Embrapa Gado de Corte, Campo Grande, Brazil.
- Pessino, S. C., J. P. A. Ortiz, O. Leblanc, C. B. Valle, C. Evans *et al.*, 1997 Identification of a maize linkage group related to apomixis in *Brachiaria*. *Theor. Appl. Genet.* 94: 439–444.
- Pessino, S. C., C. Evans, J. P. A. Ortiz, I. Armstead, C. B. Valle *et al.*, 1998 A genetic map of the apospory-region in *Brachiaria* hybrids: identification of two markers closely associated with the trait. *Hereditas* 128: 153–158.
- Prieto, P., P. Shaw, and G. Moore, 2004 Homologue recognition during meiosis is associated with a change in chromatin conformation. *Nat. Cell Biol.* 6: 906–908.
- Pupilli, F., E. J. Martinez, A. Busti, O. Calderini, C. L. Quarin *et al.*, 2004 Comparative mapping reveals partial conservation of synteny at the apomixis locus in *Paspalum* spp. *Mol. Genet. Genomics* 270: 539–548.
- Ramsey, J., and D. W. Schemske, 2002 Neopolyploidy in flowering plants. *Annu. Rev. Ecol. Syst.* 33: 589–639.
- Renvoize, S. A., W. D. Clayton, and C. H. S. Kabuye, 1996 Morphology, taxonomy and natural distribution of *Brachiaria* (Trin.) Griseb, pp. 1–15 in *Brachiaria: Biology, Agronomy, and Improvement*, edited by J. W. C. B. Miles, Valle, and B. L. Maass. CIAT, Palmira, Colombia.
- Ricci, G. C. L., A. M. Souza-Kaneshima, M. F. Felismino, A. B. Mendes-Bonato, M. S. Pagliarini *et al.*, 2011a Chromosome numbers and meiotic analysis in the pre-breeding of *Brachiaria decumbens* (Poaceae). *J. Genet.* 90: 289–294.
- Ricci, G. L., A. M. Souza-Kaneshima, M. S. Pagliarini, and C. B. Valle, 2011b Meiotic behavior in *Brachiaria humidicola* (Poaceae) hybrids. *Euphytica* 182: 355–361.
- Risso-Pascotto, C., M. S. Pagliarini, and C. B. Valle, 2005 Meiotic behavior in interspecific hybrids between *Brachiaria ruziziensis* and *Brachiaria brizantha* (Poaceae). *Euphytica* 145: 155–159.
- Risso-Pascotto, C., M. S. Pagliarini, and C. B. Valle, 2006 Microsporogenesis in *Brachiaria dictyoneura*. *Genet. Mol. Res.* 5: 837–845.
- Roche, D., Z. Chen, W. W. Hanna, and P. Ozias-Akins, 2001 Non-Mendelian transmission of an apospory-specific genomic region in a reciprocal cross between sexual pearl millet (*Pennisetum glaucum*) and an apomictic F1 (*P. glaucum* × *P. squamulatum*). *Sex. Plant Reprod.* 13: 217–223.
- Sapkota, S., J. A. Conner, W. W. Hanna, B. Simon, K. Fengler *et al.*, 2016 In silico and fluorescence in situ hybridization mapping reveals collinearity between the *Pennisetum squamulatum* apomixis carrier-chromosome and chromosome 2 of sorghum and foxtail millet. *PLoS One* 11: e0152411.
- Sears, E. R., 1976 Genetic control of chromosome pairing in wheat. *Annu. Rev. Genet.* 10: 31–51.
- Shinohara, W., Y. Ushio, A. Seo, N. Nakato, M. Kono *et al.*, 2010 Allopolyploidy in Eutetraploid and Aneutetraploid *Leposorus thunbergianus* (Polypodiaceae). *Syst. Bot.* 35: 20–29.
- Simioni, C., and C. B. Valle, 2011 Meiotic analysis in induced tetraploids of *Brachiaria decumbens* Stapf. *Crop Breed. Appl. Biotechnol.* 11: 43–49.
- Souza, V. F., M. S. Pagliarini, C. B. Valle, N. C. P. Bione, and M. U. Menon, 2015 Meiotic behavior of *Brachiaria decumbens* hybrids. *Genet. Mol. Res.* 14: 12855–12865.
- Stebbins, G. L., 1947 Types of polyploids: their classification and significance. *Adv. Genet.* 1: 403–429.
- Stebbins, G. L., 1950 *Variation and Evolution in Plants*. Columbia University Press, New York, NY.
- Stein, J., C. L. Quarin, E. J. Martínez, S. C. Pessino, and J. P. A. Ortiz, 2004 Tetraploid races of *Paspalum notatum* show polysomic inheritance and preferential chromosome pairing around the apospory-controlling locus. *Theor. Appl. Genet.* 109: 186–191.
- Stein, J., S. C. Pessino, E. J. Martínez, M. P. Rodriguez, L. A. Siena *et al.*, 2007 A genetic map of tetraploid *Paspalum notatum* Flüggé (bahiagrass) based on single-dose molecular markers. *Mol. Breed.* 20: 153–166.
- Swenne, A., B. Louant, and M. Dujardin, 1981 Induction par la colchicine de formes autotétraploïdes chez *Brachiaria ruziziensis* Germain et Evrard (Graminée). *Agron. Trop.* 36: 134–141.
- Sybenga, J., 1996 Chromosome pairing affinity and quadrivalent formation in polyploids: do segmental allopolyploids exist? *Genome* 39: 1176–1184.
- Thaikua, S., M. K. Ebina, Yamanaka, Naoki Shimoda, Katsuhisa Suenaga *et al.*, 2016 Tightly clustered markers linked to an apospory-related gene region and QTL mapping for agronomic traits in *Brachiaria* hybrids. *Grassl. Sci.* 62: 69–80.
- Valle, C. B., 1990 *Colecao de Germoplasma de Especies de Brachiaria no CIAT: Estudos Basicos Visando ao Melhoramento Genetico*. Embrapa Gado de Corte, Campo Grande, Brazil.
- Valle, C. B., and Y. H. Savidan, 1996 Genetics, cytogenetics, and reproductive biology of *Brachiaria*, pp. 147–163 in *Brachiaria: Biology, Agronomy, and Improvement*, edited by J. W. Miles, B. L. Maass, and C. B. do Valle. CIAT, Cali, Colombia.
- Valle, C. B., L. Jank, and R. M. S. Resende, 2008 Melhoramento genetico de *Brachiaria*, pp. 13–53 in *Melhoramento de Forragieras Tropicais*, edited by R. M. S. L. Resende, Jank, and C. B. Valle. Embrapa Gado de Corte, Campo Grande, Brazil.
- Van Ooijen, J. W., 2011 Multipoint maximum likelihood mapping in a full-sib family of an outbreeding species. *Genet. Res.* 93: 343–349.
- Ward, J. A., J. Bhangoo, F. Fernández-Fernández, P. Moore, J. D. Swanson *et al.*, 2013 Saturated linkage map construction in *Rubus idaeus* using genotyping by sequencing and genome-independent imputation. *BMC Genomics* 14: 2.
- Worthington, M. L., and J. W. Miles, 2015 Reciprocal full-sib recurrent selection and tools for accelerating genetic gain in apomictic *Brachiaria*, pp. 19–30 in *Molecular Breeding of Forage and Turf*, edited by H. Budak, and G. Spangenberg. Springer International, Cham, Switzerland.
- Zhang, G., X. Liu, Z. Quan, S. Cheng, X. Xu *et al.*, 2012 Genome sequence of foxtail millet (*Setaria italica*) provides insights into grass evolution and biofuel potential. *Nat. Biotechnol.* 30: 549–554.
- Zorzatto, C., L. Chiari, G. Araújo Bitencourt, C. B. Valle, G. O. Campos Leguizamón *et al.*, 2010 Identification of a molecular marker linked to apomixis in *Brachiaria humidicola* (Poaceae). *Plant Breed.* 129: 734–736.

Communicating editor: A. Houben

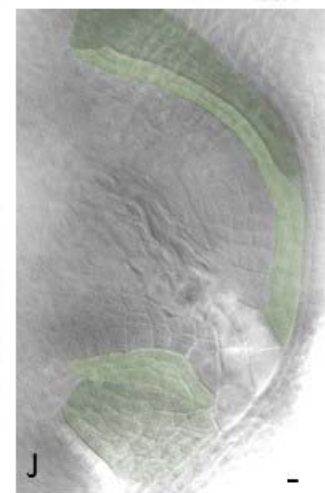
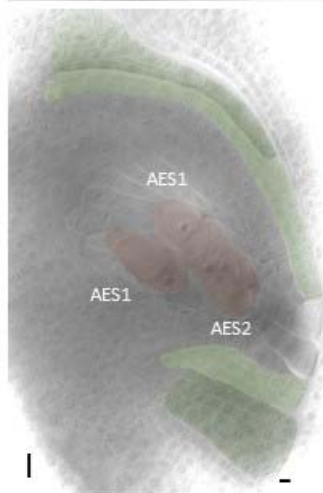
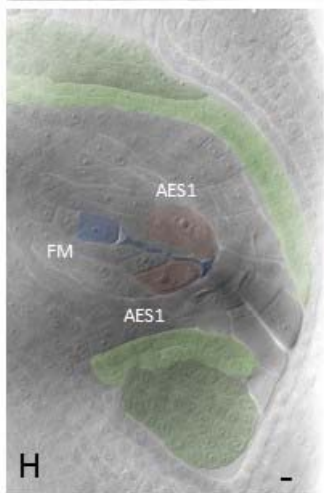
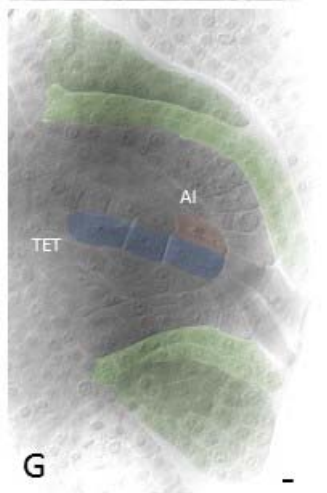
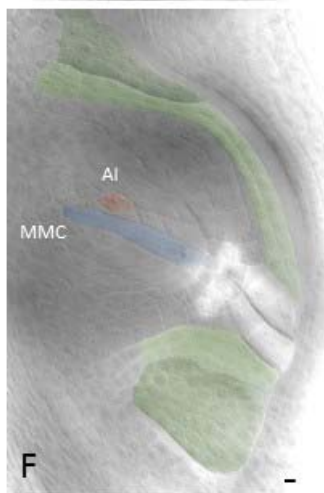
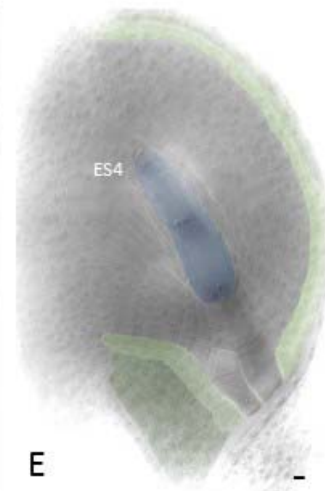
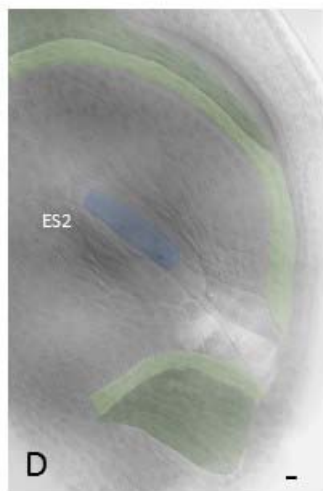
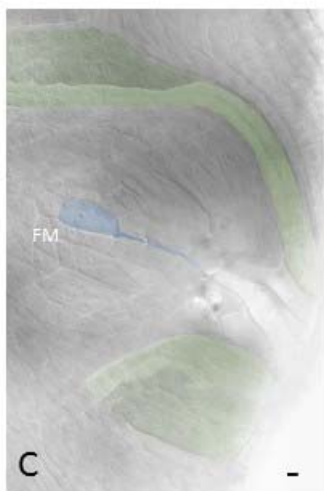
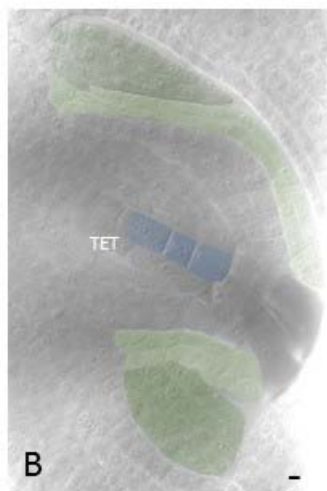
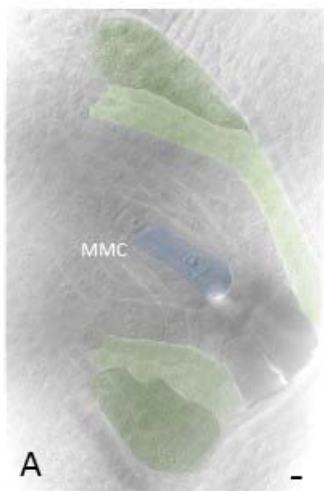
GENETICS

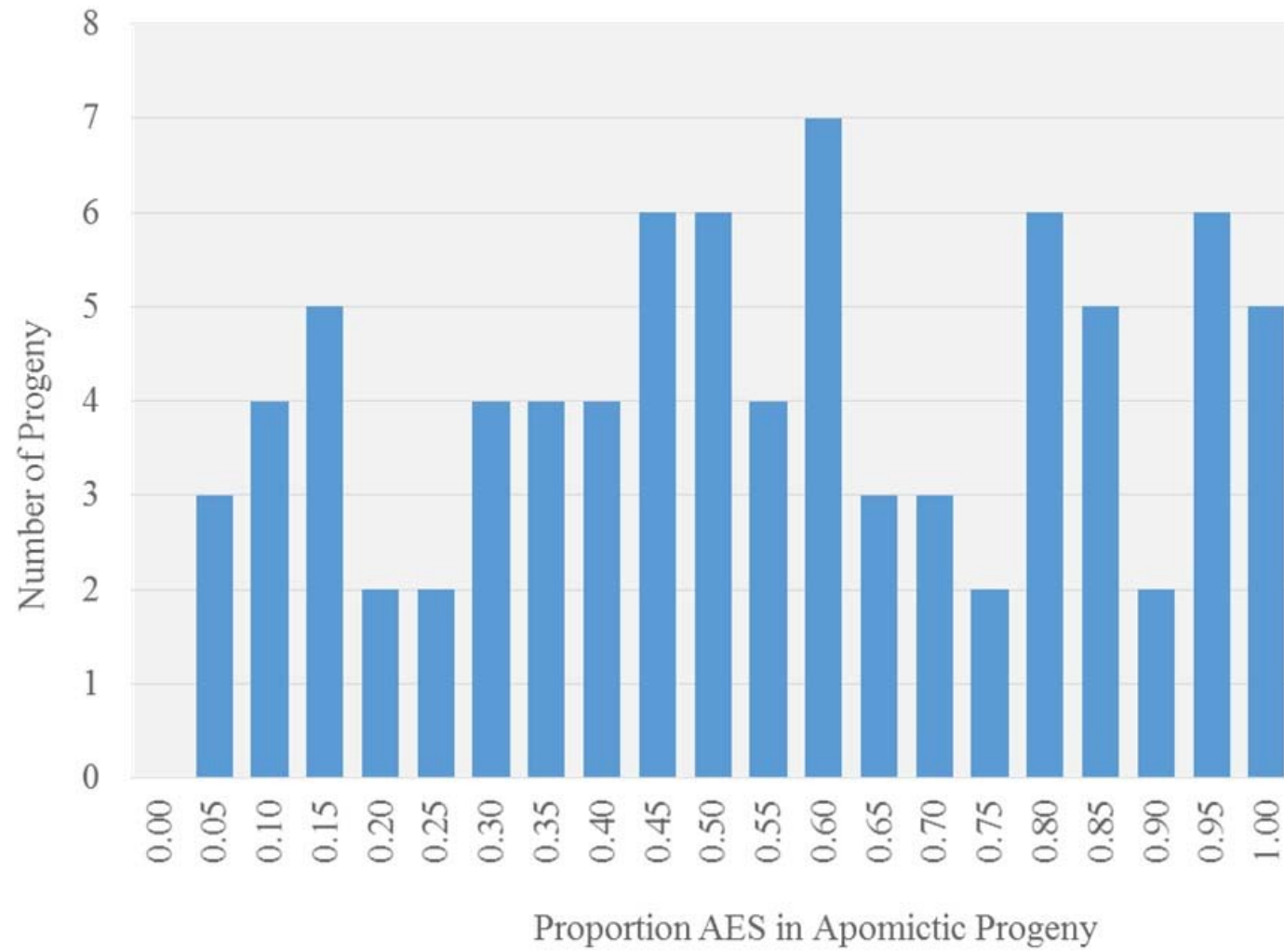
Supporting Information

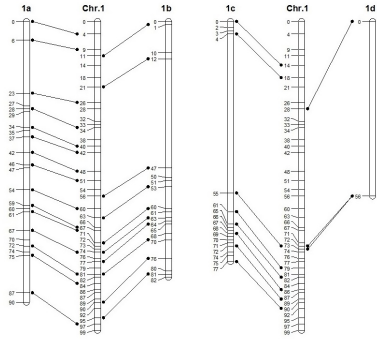
www.genetics.org/lookup/suppl/doi:10.1534/genetics.116.190314/-/DC1

A Parthenogenesis Gene Candidate and Evidence for Segmental Allopolyploidy in Apomictic *Brachiaria decumbens*

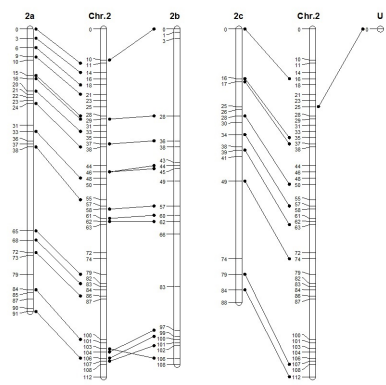
Margaret Worthington, Christopher Heffelfinger, Diana Bernal, Constanza Quintero, Yeny Patricia Zapata,
Juan Guillermo Perez, Jose De Vega, John Miles, Stephen Dellaporta, and Joe Tohme



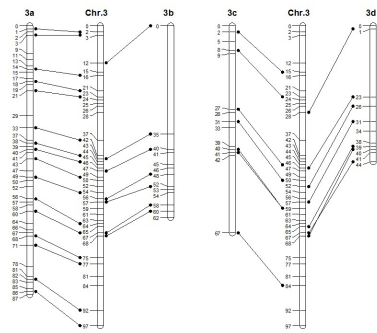




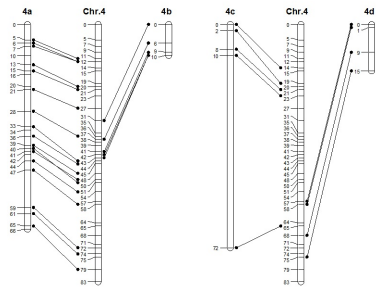
A *B. ruzizensis* Chr. 1



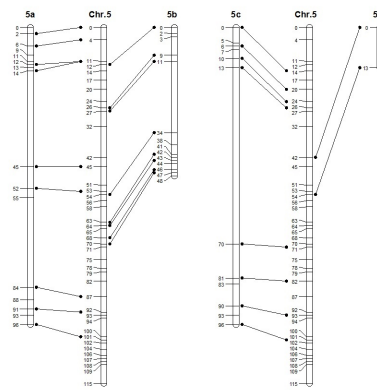
B *B. ruzizensis* Chr. 2



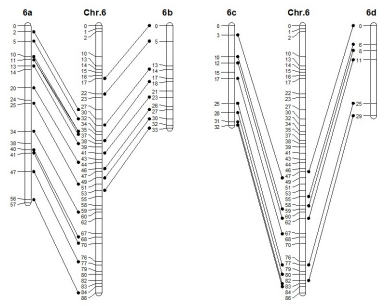
C *B. ruzizensis* Chr. 3



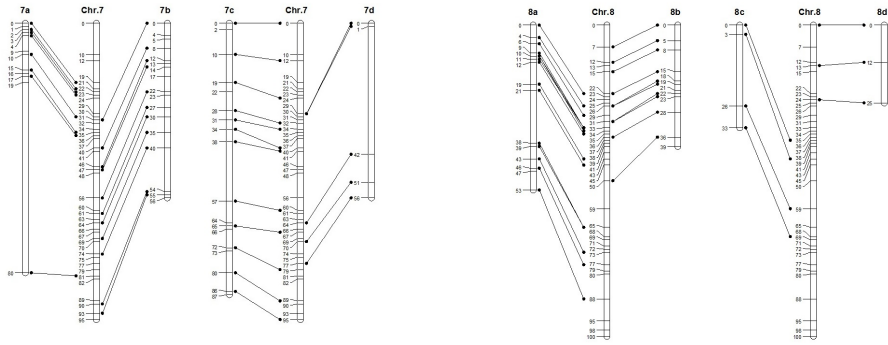
D *B. ruzizensis* Chr. 4



E *B. ruzizensis* Chr. 5

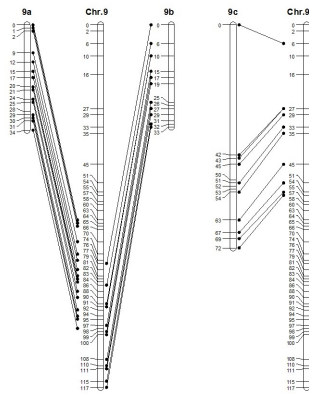


F *B. ruzizensis* Chr. 6



G *B. ruziziensis* Chr. 7

H *B. ruziziensis* Chr. 8



I *B. ruziziensis* Chr. 9

Figure S3 Comparison of individual *B. ruziziensis* haplotype maps with the combined genetic map of each chromosome (A-I). The four homologous linkage groups corresponding to each chromosome are labeled a-d. *Brachiaria ruziziensis* chromosomes 2 and 9 had only three corresponding linkage groups in the maternal haplotype map. One previously unlinked marker (U) maps to chromosome 2 based on shared linkages with double dose alleles and synteny analysis. Map distances are given in Kosambi cM. Marker names and positions are given in Tables S7-S9.

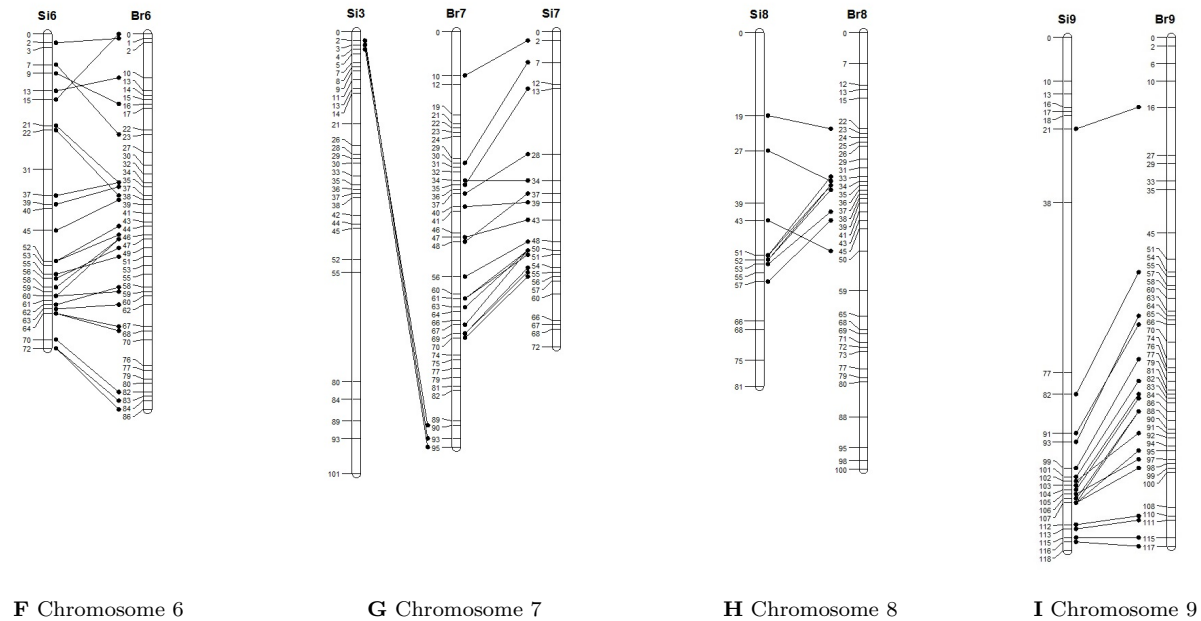
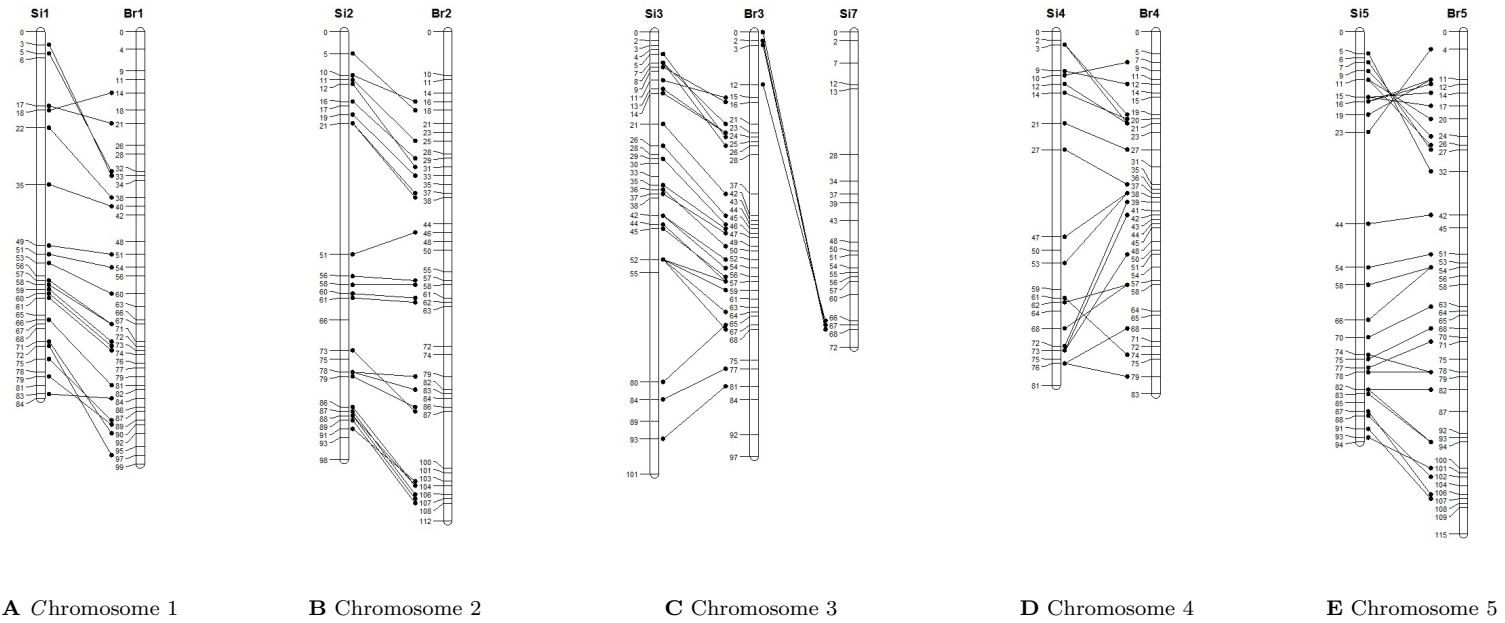
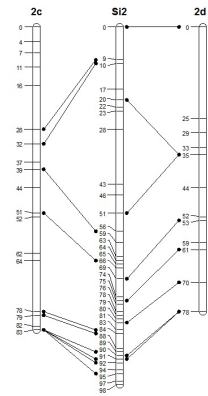
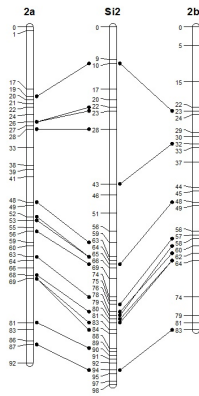
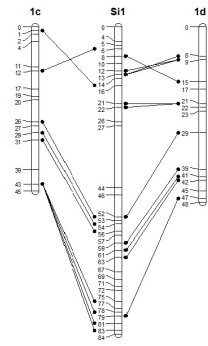
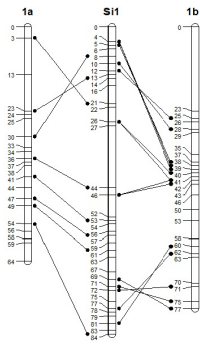
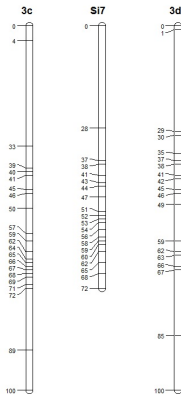
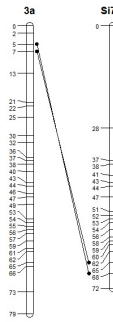
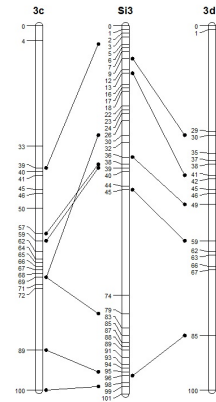
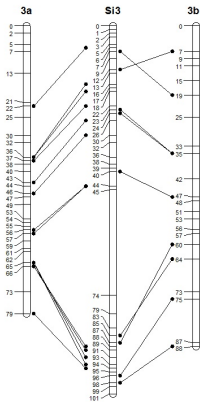


Figure S4 Comparison of the combined genetic maps of each *Brachiaria ruziziensis* BRX 44-02 chromosome (A-I) with the physical maps of syntenous *Setaria italica* chromosomes. The *B. ruziziensis* genetic maps are labeled Br1-Br9, while the *S. italica* physical maps are labeled Si1-9. C and G show a reciprocal translocation between chromosomes 3 (0-2 Mbp) and 7 (33-36 Mbp). One unit on the physical map reflects 5×10^5 bp. Genetic positions are given in Kosambi cM. Marker names and positions are given in Table S9.



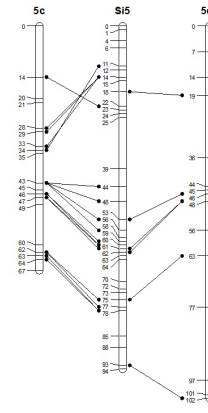
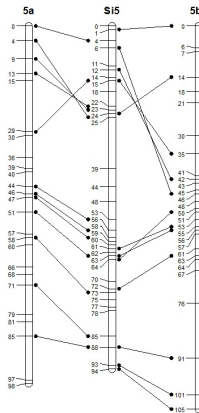
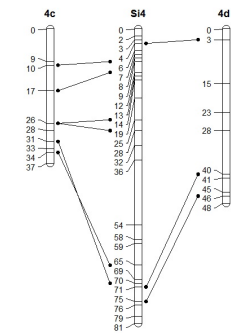
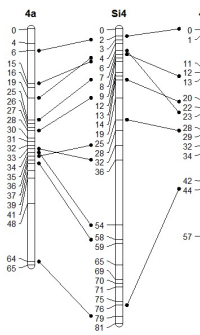
A Chromosome 1

B Chromosome 2



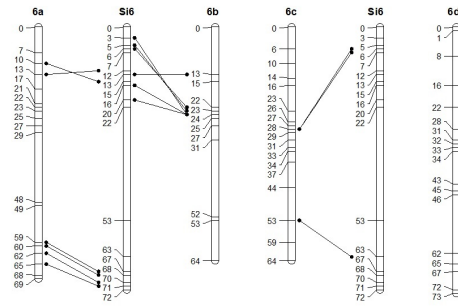
C Chromosome 3

D Chromosome 3

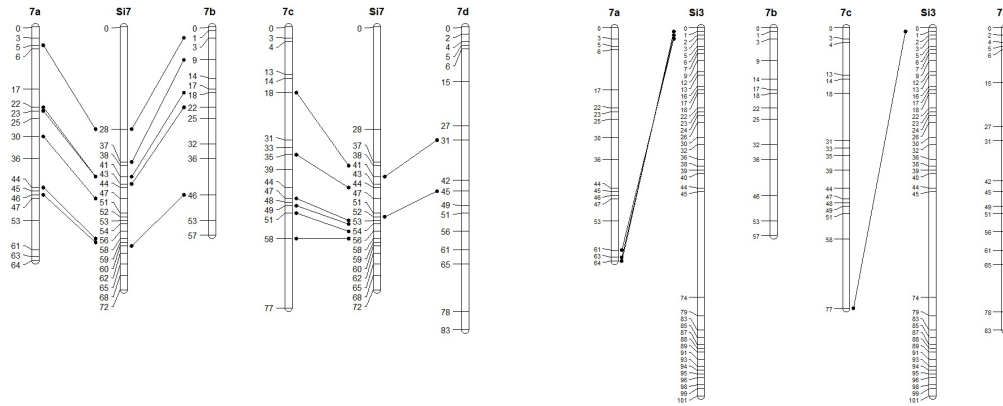


E Chromosome 4

F Chromosome 5

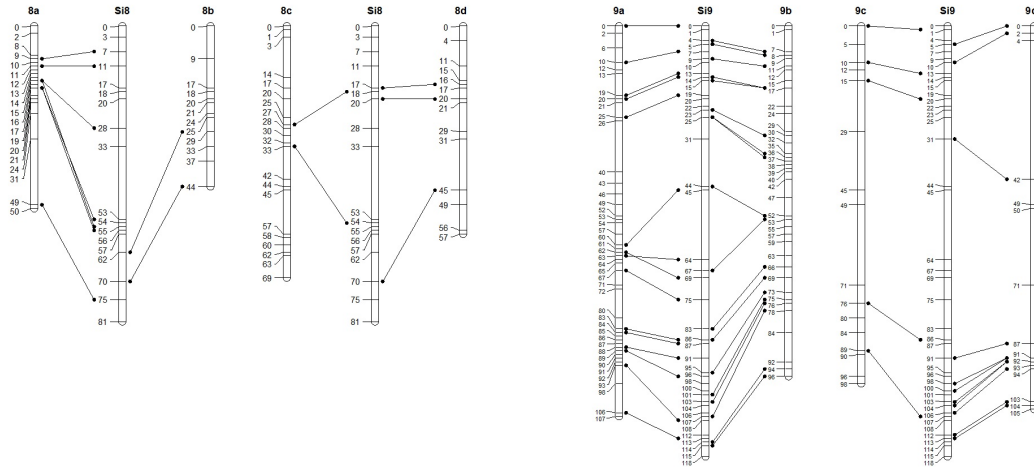


G Chromosome 6



H Chromosome 7

I Chromosome 7



J Chromosome 8

K Chromosome 9

Figure S5 Comparison of the four haplotype maps of each *Brachiaria decumbens* CIAT 606 chromosome (A-K) with the physical maps of syntenous *Setaria italica* chromosomes. The *B. decumbens* haplotype maps for each chromosome are labeled a-d, while the *S. italica* physical maps are labeled Si1-9. Figures C-D and H-I show a reciprocal translocation between chromosomes 3 (0-2 Mbp) and 7 (33-36 Mbp). One unit on the physical map reflects 5×10^5 bp. Genetic positions are given in Kosambi cM. Marker names and positions are given in Table S7.

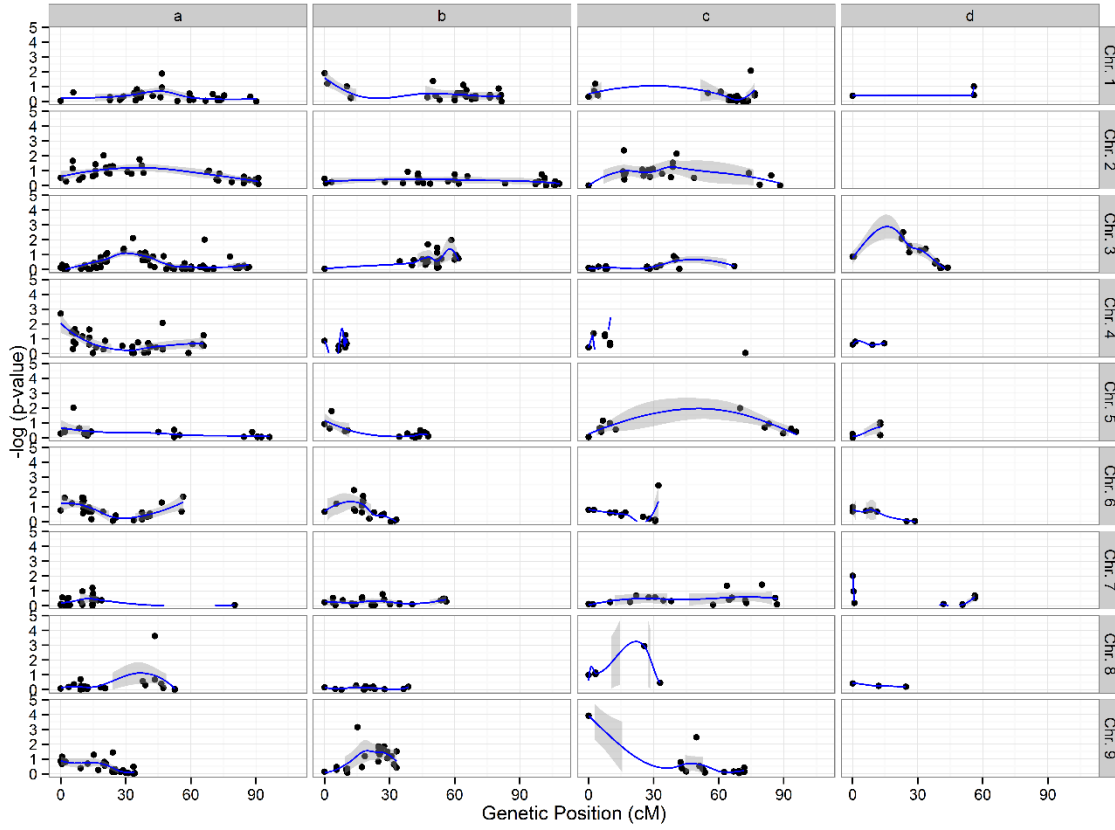
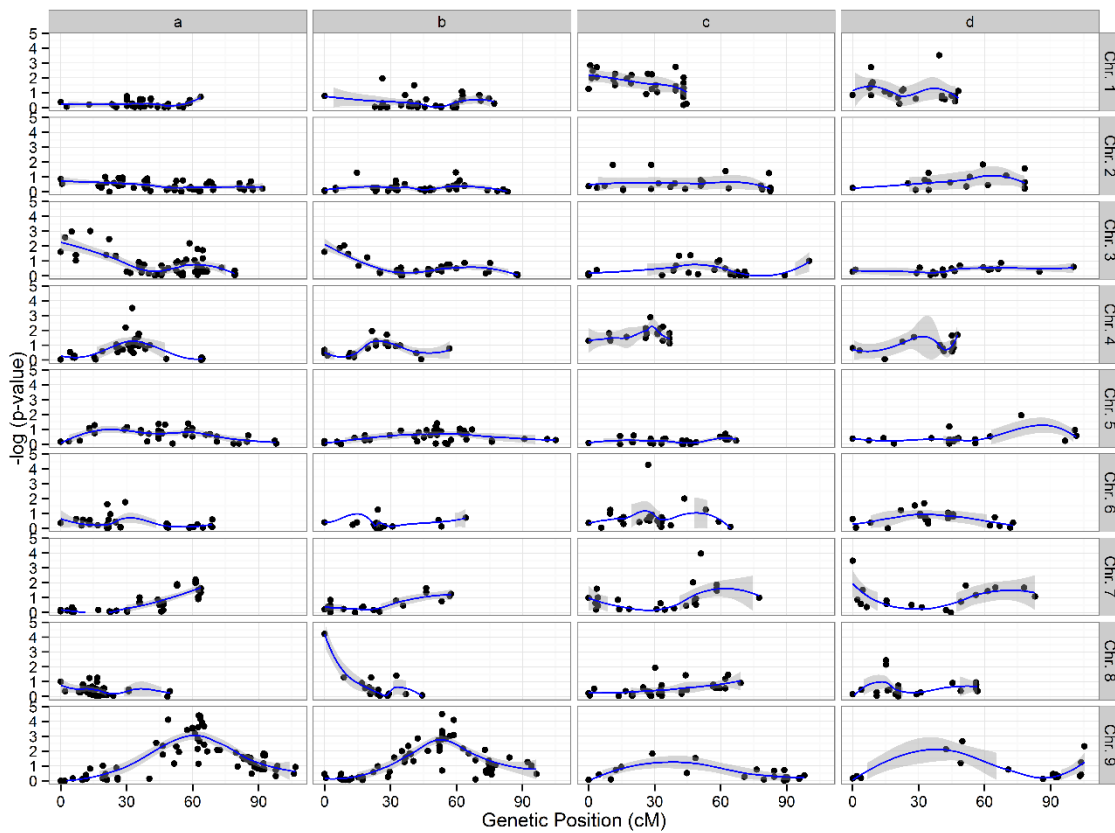
A**B**

Table S1. Depth of genotyping-by-sequencing read coverage in the parents and F1 progeny of the BRX 44-02 x CIAT 606 mapping population. (.xlsx, 14 KB)

www.genetics.org/lookup/suppl/doi:10.1534/genetics.116.190314/-/DC1/TableS1.xlsx

Table S2. Primer sequences for six Kompetitive allele specific PCR (KASP) markers designed from Genotyping-by-Sequencing (GBS) markers linked to the apospory specific genetic region in the BRX 44-02 x CIAT 606 mapping population. (.xlsx, 10 KB)

www.genetics.org/lookup/suppl/doi:10.1534/genetics.116.190314/-/DC1/TableS2.xlsx

Table S3. Genotype scores of p779/p780, N14, KASP, and GBS-derived SDA and DDA markers evaluated in the BRX 44-02 x CIAT 606 population (a = homozygote, h = heterozygote, and - = missing data). (.xlsx, 1,343 KB)

www.genetics.org/lookup/suppl/doi:10.1534/genetics.116.190314/-/DC1/TableS3.xlsx

Table S4. UNEAK sequences of the GBS derived SDA and DDA markers with variant alleles designated as 'query' and 'hit' according to Lu et al. (2013). (.xlsx, 133 KB)

www.genetics.org/lookup/suppl/doi:10.1534/genetics.116.190314/-/DC1/TableS4.xlsx

Table S5. Reproductive mode, total number of pistils evaluated, number of pistils with abnormal embryo sacs, proportion of pistils with only sexual (Polygonum type) embryo sacs, and average number of embryo sacs per pistil in the parents and F1 progeny of the BRX 44-02 x CIAT 606 mapping population. (.xlsx, 16 KB)

www.genetics.org/lookup/suppl/doi:10.1534/genetics.116.190314/-/DC1/TableS5.xlsx

Table S6. Number of Genotype-by-Sequencing (GBS) derived single-nucleotide polymorphism (SNP) markers in datasets with various thresholds for missing genotype calls and mean percentage of missing genotype calls in each dataset. (.xlsx, 10 KB)

[www.genetics.org/lookup/suppl/ doi:10.1534/genetics.116.190314/-/DC1/TableS6.xlsx](http://www.genetics.org/lookup/suppl/doi:10.1534/genetics.116.190314/-/DC1/TableS6.xlsx)

Table S7. Single dose allele marker positions in the BRX 44-02 and CIAT 606 parental linkage maps, physical positions on the *S. italica* reference genome, deviations from the expected 1:1 ratio of heterozygotes to homozygotes in the F1 progeny, and ratio of segregating allele reads to total reads in the heterozygous parent. (.xlsx, 218 KB)

www.genetics.org/lookup/suppl/doi:10.1534/genetics.116.190314/-/DC1/TableS7.xlsx

Table S8. Double dose allele (DDA) markers heterozygous in BRX 44-02 and CIAT 606, single dose allele (SDA)-DDA linkages with markers mapped to Brachiaria chromosomes 1-9, unique physical positions on the *Setaria italica* reference genome, and deviations from the expected 5:1 ratio of heterozygotes to homozygotes in the F1 progeny. (.xlsx, 31 KB)

www.genetics.org/lookup/suppl/doi:10.1534/genetics.116.190314/-/DC1/TableS8.xlsx

Table S9. Combined linkage maps for *B. ruziziensis* chromosomes 1-9 created based on linkages between single dose allele (SDA) and double dose allele (DDA) markers, presented with original marker positions on the SDA haplotype maps and physical positions on the *Setaria italica* reference genome. (.xlsx, 34 KB)

[www.genetics.org/lookup/suppl/ doi:10.1534/genetics.116.190314/-/DC1/TableS9.xlsx](http://www.genetics.org/lookup/suppl/doi:10.1534/genetics.116.190314/-/DC1/TableS9.xlsx)

Table S10. Segregation of alleles within the *B. decumbens* genetic map. (.xlsx, 10,151 KB)

www.genetics.org/lookup/suppl/doi:10.1534/genetics.116.190314/-/DC1/TableS10.xlsx

Table S11. A diversity panel (n = 162) composed of four apomictic interspecific *Brachiaria* hybrid cultivars and accessions of *Brachiaria brizantha* (n = 82), *B. decumbens* (n = 13), *B. ruziziensis* (n = 11), and *B. humidicola* (n = 52) with a mixture of apomictic, sexual, and unknown reproductive mode from the CIAT genetic resources program forages collection evaluated with the ASGR-linked KASP markers K42517, K62444, K76831, K207542; the SCAR marker N14; and the ASGR-BBML specific primers p779/p780.

www.genetics.org/lookup/suppl/doi:10.1534/genetics.116.190314/-/DC1/TableS11.xlsx

File S1

List of Supplemental Figures and Tables

Supplemental figures

Figure S1 Representative sexual (A-E) and apomictic (F-I) embryo sacs observed in F₁ progeny of the BRX 44-02 x CIAT 606 mapping population. Outer and inner integuments are shaded dark and light green. Sexual and apomictic reproductive cells are shaded blue and orange. Panel J shows an abnormal embryo sac, which has melded membranes. Scale bars represent 10 μ m. Different focal planes were stitched together as needed to show all relevant reproductive cells within a single pistil. Abbreviations: megaspore mother cell (MMC), tetrad (TET), functional megaspore (FM), embryo sac with two nuclei (ES2), embryo sac with four nuclei (ES4), aposporic initial (AI), aposporic embryo sac with one nucleus (AES1), aposporic embryo sac with two nuclei (AES2).

Figure S2 Distribution of proportion of apomictic embryo sacs (AES) among the 83 apomictic F₁ progeny from the BRX 44-02 x CIAT 606 mapping population as determined by embryo sac analysis of at least 30 normally developed ovaries per genotype.

Figure S3 Comparison of individual *B. ruziziensis* haplotype maps with the combined genetic map of each chromosome (A-I). The four homologous linkage groups corresponding to each chromosome are labeled a-d. *Brachiaria ruziziensis* chromosomes 2 and 9 had only three corresponding linkage groups in the maternal haplotype map. One previously unlinked marker (U) belongs to chromosome 2 based on shared linkages with double dose alleles and synteny analysis. Map distances are given in Kosambi cM. Marker names and positions are given in Tables S7-S9.

Figure S4 Comparison of the combined genetic maps of each *Brachiaria ruziziensis* BRX 44-02 chromosome (A-I) with the physical maps of syntenous *Setaria italica* chromosomes. The *B. ruziziensis* genetic maps are labeled Br1-9, while the *S. italica* physical maps are labeled Si1-9. C and G show a reciprocal translocation between chromosomes 3 (0-2 Mbp) and 7 (33-36 Mbp). One unit on the physical map reflects 5×10^5 bp. Genetic positions are given in Kosambi cM. Marker names and positions are given in Table S9.

Figure S5 Comparison of the four haplotypes maps of each *Brachiaria decumbens* CIAT 606 chromosome (A-K) with the physical maps of syntenous *Setaria italica* chromosomes. The *B. decumbens* haplotype maps for each chromosome are labeled a-d, while the *S. italica* physical maps are labeled Si1-9. Figures C-D and H-I show a reciprocal translocation between chromosomes 3 (0-2 Mbp) and 7 (33-36 Mbp). One unit on the physical map reflects 5×10^5 bp. Genetic positions are given in Kosambi cM. Marker names and positions are given in Table S7.

Figure S6 Segregation distortion of markers mapped to haplotypes (a-d) of the nine chromosomes in the (A) BRX 44-02 maternal linkage map and (B) CIAT 606 paternal linkage map. Markers were classified as single dose alleles and selected for mapping based on having a segregation ratio of less than 2:1 (heterozygotes to homozygotes) in the F_1 progeny and less than 20% missing data. Markers were tested for deviation from the expected allelic ratio of 1:1 by χ^2 test. The log-transformed p-values [$-\log(\text{p-value})$] obtained from χ^2 tests and locally weighted scatterplot smoothing (LOESS) lines were plotted against the genetic positions of mapped markers.

Supplemental tables

Table S1 Depth of genotyping-by-sequencing read coverage in the parents and F1 progeny of the BRX 44-02 x CIAT 606 mapping population.

Table S2 Primer sequences for six Kompetitive allele specific PCR (KASP) markers designed from genotyping-by-sequencing (GBS) markers linked to the apospory-specific genomic region in the BRX 44-02 x CIAT 606 mapping population.

Table S3 Genotype scores of p779/p780, N14, KASP, and GBS-derived SDA and DDA markers evaluated in the BRX 44-02 x CIAT 606 population (a = homozygote, h = heterozygote, and - = missing data).

Table S4 UNEAK sequences of the GBS derived SDA and DDA markers with variant alleles designated as 'query' and 'hit' according to Lu *et al.* (2013).

Table S5 Reproductive mode, total number of pistils evaluated, number of pistils with abnormal embryo sacs, proportion of pistils with only sexual (*Polygonum* type) embryo sacs, and average number of embryo sacs per pistil in the parents and F₁ progeny of the BRX 44-02 x CIAT 606 mapping population.

Table S6 Number of genotyping-by-sequencing (GBS) derived single-nucleotide polymorphism (SNP) markers in datasets with various thresholds for missing genotype calls and mean percentage of missing genotype calls in each dataset.

Table S7 Single dose allele marker positions in the BRX 44-02 and CIAT 606 parental linkage maps, physical positions on the foxtail millet (*Setaria italica*) reference genome, deviations from the expected 1:1 ratio of heterozygotes to homozygotes in the F₁ progeny, and ratio of segregating allele reads to total reads in the heterozygous parent.

Table S8 Double dose allele (DDA) markers heterozygous in BRX 44-02 and CIAT 606, single dose allele (SDA)-DDA linkages with markers mapped to *Brachiaria* chromosomes 1-9, physical positions on the *Setaria italica* reference genome, and deviations from the expected 5:1 ratio of heterozygotes to homozygotes in the F1 progeny.

Table S9 Combined linkage maps for *B. ruziziensis* chromosomes 1-9 created based on linkages between single dose allele (SDA) and double dose allele (DDA) markers, presented with original marker positions on the SDA haplotype maps and physical positions on the *Setaria italica* reference genome.

Table S10 Segregation of alleles within the *B. decumbens* genetic map. Marker pairs with statistically significant segregation and co-segregation interactions based on Fisher's exact test for count data are respectively colored orange and blue.

Table S11 A diversity panel (n = 162) composed of four apomictic interspecific *Brachiaria* hybrid cultivars and accessions of *Brachiaria brizantha* (n = 81), *B. decumbens* (n = 13), *B. ruziziensis* (n = 12), and *B. humidicola* (n = 52) with a mixture of apomictic, sexual, and unknown reproductive mode from the CIAT genetic resources program forages collection evaluated with the ASGR-linked KASP markers K42517, K62444, K76831, K207542; the SCAR marker N14; and the ASGR-BBML specific primers p779/p780. Five putatively sexual progeny of the synthetic autotetraploid *Panicum maximum* accession Tift SPM92 (PI 570664; Hanna and Nakagawa 1994), and five accessions each of *Cenchrus ciliaris* and *P. maximum* were also evaluated with N14 and p779/p780.

Supplemental figures and tables literature cited

- Dusi, D. M. A., and M. T. M. Willemse, 1999 Apomixis in *Brachiaria decumbens* Stapf: gametophytic development and reproductive calendar. *Acta. Biol. Cracov. Ser. Bot.* 41: 151–162.
- Hanna, W. W., and H. Nakagawa, 1994 Registration of Tift SPM92 Sexual Guineagrass Germplasm. *Crop Sci.* 34: 547.
- Jungmann, L., B. B. Z. Vigna, K. R. Boldrini, a C. B. Sousa, C. B. Valle et al., 2010 Genetic diversity and population structure analysis of the tropical pasture grass *Brachiaria humidicola* based on microsatellites, cytogenetics, morphological traits, and geographical origin. *Genome* 53: 698–709.
- Lu, F., A. E. Lipka, J. Glaubitz, R. Elshire, J. H. Cherney et al., 2013 Switchgrass Genomic Diversity, Ploidy, and Evolution: Novel Insights from a Network-Based SNP Discovery Protocol. *PLoS Genet.* 9: e1003215.
- Mendes-Bonato, A. B., M. S. Pagliarini, F. Forli, C. B. Valle, and M. I. O. Penteadó, 2002 Chromosome numbers and microsporogenesis in *Brachiaria brizantha* (Gramineae). *Euphytica* 125: 419–425.
- Ortega, L. A. F., 1995 Caracterización del modo reproductivo de tres especies del género *Brachiaria* (Trin.) Griseb. [Thesis]. Universidad del Cauca, Popayan, Colombia.
- Penteadó, M., A. dos Santos, I. F. Rodrigues, C. B. Valle, M. Seixas et al., 2000 Determinação de ploidia e avaliação da quantidade de DNA total em diferentes espécies do género *Brachiaria*. Embrapa Gado de Corte, Campo Grande, Brazil.

- Rodrigues, J. C. M., G. B. Cabral, D. M. A. Dusi, L. V. De Mello, D. J. Rigden et al., 2003
Identification of differentially expressed cDNA sequences in ovaries of sexual and
apomictic plants of *Brachiaria brizantha*. *Plant Mol. Biol.* 53: 745–757.
- Swenne, A., B. Louant, and M. Dujardin, 1981 Induction par la colchicine de formes
autotétraploïdes chez *Brachiaria ruziziensis* Germain et Evrard (Graminée). *Agron. Trop.*
36: 134–141.
- Valle, C. B., 1990 Colecao de germoplasma de especies de *Brachiaria* no CIAT: Estudos basicos
visando ao melhoramento genetico. Embrapa Gado de Corte, Campo Grande, Brazil.
- Valle, C. B., L. Jank, and R. M. S. Resende, 2008 Melhoramento genetico de *Brachiaria*, pp. 13–
53 in *Melhoramento de forragieras tropicais*, edited by R. M. S. Resende, L. Jank, and C.
B. Valle. Embrapa Gado de Corte, Campo Grande, Brazil.
- Valle, C. B., Y. H. Savidan, and L. Jank, 1989 Apomixis and sexuality in *Brachiaria decumbens*
Stapf, pp. 407–408 in XVI International Grassland Congress, INRA, Nice, France.
- Vigna, B. B., G. C. Alleoni, L. Jungmann, C. B. Valle, and A. P. Souza, 2011 New microsatellite
markers developed from *Urochloa humidicola* (Poaceae) and cross amplification in
different *Urochloa* species. *BMC Res. Notes* 4: 523.

File S2

Supplemental materials and methods

Mapping population

A synthetic sexual autotetraploid plant (*B. ruziziensis* BRX 44-02) was crossed to an apomictic pollen donor (*B. decumbens* CIAT 606) to generate an F₁ mapping population with 169 progeny. The female parent of the mapping population, BRX 44-02, was the original source of sexuality in the CIAT hybrid *Brachiaria* breeding program. The first synthetic sexual autotetraploids were generated by doubling the chromosome number of a diploid sexual accession collected in the Ruzizi plains of Burundi using colchicine (Swenne *et al.* 1981). The various tetraploid plants derived from colchicine doubling were then crossed to each other by open pollination to form progeny including the female parent of this cross, BRX 44-02. The male parent of the cross, CIAT 606 (cv. Basilisk; also known as BRA-001058, CPI-001694, CPI-006798, EBC-D062, and ILCA-1087), is a popular commercial cultivar selected from an unmodified germplasm accession collected in Uganda (Oram 1990).

Embryo Sac Analysis

Inflorescences for embryo sac analysis were harvested from parents and progeny grown in 25 cm diameter pots in screen house conditions at CIAT in Palmira, Colombia (1001 masl; 3.5833° N, 76.2500° W). Not all progeny could be induced to flower in Palmira, so an additional clonal replicate was moved to a higher altitude site in Popayán, Colombia (1760 masl; 2.4542° N, 76.6092° W), where cooler nighttime temperatures stimulate flowering in *Brachiaria*. Two F₁ progeny could not be induced to flower in either environment and were excluded from embryo sac analysis. Multiple inflorescences from parents and F₁ progeny were collected in the boot

23 stage and fixed using formal acetic acid (FAA) for 48 hours. Samples were then stored in 70%
24 ETOH, which was exchanged every 24 hours for three days to remove residual formaldehyde.

25 Pistils corresponding to Dusi and Willemse (1999) developmental stages 3-8 were excised
26 under a dissecting microscope. Excised pistils were stored in 95% ETOH, which was exchanged
27 every 24 hours for three days to remove all water. Next, pistils were cleared by successive
28 transfer to solutions of 100% ethanol, 2:1 (v:v) 95% ethanol:benzyl benzoate, 1:2 (v:v) 95%
29 ethanol:benzyl benzoate, and two separate solutions of 2:1 benzyl benzoate:dibutyl phthalate at
30 intervals greater than six hours. The cleared pistils were inserted into notches of saw-tooth cut 5
31 x 35 mm pieces of index cards, such that the ovules showed a sagittal optical section when
32 observed under differential interference contrast (DIC) microscopy. Index cards were glued to
33 glass slides and dampened with clearing solution before inserting pistils. After all notches were
34 loaded, more clearing solution was added to fill the notches and slides were covered with a 22 x
35 50 mm glass coverslip.

36 Abnormal (degenerated or ruptured) pistils are frequently observed in both apomictic and
37 sexual *Brachiaria* plants (Valle *et al.* 1989). The number of abnormal pistils was recorded for
38 each of the progeny, and such pistils were excluded from further analyses. The total number of
39 embryo sacs and developmental stage of each embryo sac were also recorded for each pistil. In
40 apomictic plants the total number of embryo sacs per pistil could only be evaluated for pistils in
41 (Dusi and Willemse 1999) growth stages 3-4, as it is very difficult to distinguish individual
42 aposporic embryo sacs at later stages using DIC microscopy (Lutts *et al.* 1994). Sexual
43 (*Polygonum* type) embryo sacs were observed in the megaspore mother cell, dyad, tetrad,
44 functional megaspore, and embryo sac with one, two, and four nuclei developmental stages while

45 apomictic (*Panicum* type) embryo sacs were observed at the aposporic initial and aposporic
46 embryo sac with one or two nuclei developmental stages (Fig. S1). Progeny with pistils showing
47 only Polygonum type embryo sac development were scored as sexual, while progeny with any
48 pistils that had enlarged vacuolated nucellar cells or further *Panicum* type embryo sac
49 development were scored as apomictic. A Chi Squared test was then performed to evaluate
50 whether the population fit the expected segregation ratio (1:1 apomictic:sexual) for monogenic
51 inheritance of the ASGR. Potential differences in the number of embryo sacs per pistil in
52 apomictic and sexual progeny were compared by analysis of variance (ANOVA) in SAS 9.2
53 (SAS Institute Inc., Cary, NC).

54 ***GBS library preparation and sequencing***

55 Tissue for DNA extractions was harvested from young leaves of parents and progeny grown in
56 greenhouse conditions at CIAT. Genomic DNA was isolated according to the Shure *et al.* (1983)
57 urea-phenol extraction protocol with slight modifications. Quality and quantity of dsDNA was
58 assessed prior to GBS library construction with Quant-iT™ PicoGreen® dsDNA Assay Kit
59 (ThermoFisher) in a microplate reader Synergy H1m (Biotek). Libraries were prepared following
60 Heffelfinger *et al.* (2014). Briefly, 500 ng of DNA from each genotype was hybridized onto
61 AMPure XL Solid Phase Reversible Immobilization (SPRI) beads (AG3880, Beckman Coulter),
62 washed following the Broad Institute protocol (Fisher *et al.* 2011), and digested with the partially
63 methylation sensitive four base pair cutting restriction enzyme HINCII (R0103, New England
64 Biolabs) for two hours following manufacturer's guidelines. Following digestion, samples were
65 immobilized to SPRI beads, washed, and processed with dA tailing to ensure compatibility with
66 standard adaptors and prevent concatamer formation. Samples were then washed again and
67 ligated to standard Illumina Y-adaptors using the Quick T4 DNA ligase kit (M0202M, New

68 England Biolabs). In-solution size selection was performed in microtiter plates using SPRI
69 methodology following the Broad Institute protocol (Fisher *et al.* 2011). Barcodes (FC-121-
70 1003, Illumina) were added using a primer-based method that adds dual indices to the ends of
71 adaptor ligated DNA fragments in a low-cycle PCR step as described by Heffelfinger *et al.*
72 (2014). Mapping population and parental libraries were sequenced as 75 bp paired-end reads on
73 the Illumina HiSeq 2500 by the Yale Center for Genome Analysis
74 (<http://medicine.yale.edu/keck/ycga/index.aspx>) following the manufacturer's protocol. Final
75 depths of sequencing coverage (75 bp reads) are provided in Table S1.

76 ***Sequence analysis and GBS SNP genotype calling***

77 *De novo* SNP discovery and genotype calling was conducted using the Tassel 3.0 Universal
78 Network Enabled Analysis Kit (UNEAK) pipeline (Lu *et al.* 2013). To make the GBS
79 sequencing datasets compatible with UNEAK, a false ApeKI restriction site and sample-unique
80 barcode were added *in silico* to the start of each read using custom scripts. Reads were then
81 quality filtered, de-multiplexed, and trimmed to 64 bp in the initial step of the UNEAK pipeline.
82 Identical reads were then collapsed into tags, and each tag with 10 or more reads was retained for
83 pairwise alignment. Pairs of tags that differed at a single nucleotide position were called as
84 candidate SNPs. A network filter was then used to discard likely repeats, paralogs, and error
85 tags. A greater number of reads are required to make accurate genotypic calls in tetrasomic
86 polyploid populations than diploid populations. Thus, strict genotype calling thresholds were
87 employed following the recommendations of Li *et al.* (2014) in order to reliably distinguish
88 between homozygotes (AAAA) and triplex heterozygotes (AAAB). Briefly, 11 or more reads of
89 a single allele were required to call a homozygote, and at least two reads per allele and a
90 minimum minor allele frequency greater than 0.10 were required to call a heterozygote genotype.

91 If conditions for homozygote or heterozygote genotype calling were not met, a missing genotype
92 call was assigned. No attempt was made to score dosage and distinguish among the three
93 heterozygote genotypes possible in an autotetraploid in the F₁ progeny. The ratio of the number
94 of reads of the segregating allele to the total read number (segregating allele read frequency) for
95 each marker was calculated in both parents to evaluate potential differentiation of sub-genomes.

96 ***KASP assay development and validation***

97 Six Kompetitive Allele Specific PCR (KASP) assays (K42517, K62444, K76831, K100912,
98 K171196, and K207542) were designed based on flanking markers TP42517, TP62444,
99 TP76831, TP100912, TP171196, and TP207542, which mapped to within 13 cM proximal and 4
100 cM distal of the ASGR on the CIAT 606 parental map (Table S2). All six KASP assays were
101 validated with the full mapping population and parents, and the four most tightly linked markers
102 (K42517, K62444, K76831, and K207542) were also used to evaluate a diversity panel (n = 162)
103 composed of four interspecific apomictic hybrid cultivars and accessions of *B. brizantha* (n =
104 81), *B. decumbens* (n = 13), *B. ruziziensis* (n = 12), and *B. humidicola* (n = 52) with a mixture of
105 apomictic, sexual, and unknown reproductive mode from the CIAT genetic resources program
106 forages collection (<http://isa.ciat.cgiar.org/>). Genomic DNA for marker analysis was isolated
107 with a modified MATAB-Chloroform protocol following Risterucci *et al.* (2000). Quality and
108 quantity of DNA samples were measured by Absorbance using a Take™3TRIO Micro-volume
109 plate in a microplate reader Synergy H1m (Biotek). Marker reactions were conducted using
110 LGC's genotyping service (LGC Genomics, Beverly, MA) in 4 µL reaction system including 2
111 µL low rox KASP master mix, 0.106 µL of primer mix (0.318 µL of each primer at final
112 concentration), and 2 µL of 10-25 ng/µl genomic DNA. The PCR conditions for the KASP
113 marker assays were 94°C for 15 min, followed by 10 cycles of touch down PCR from 68°C to

114 60°C with 0.8°C decrease per cycle, then followed by 30 cycles of 94°C for 20 s and 57°C for 1
115 min. PCR fluorescent endpoint readings were performed using the Light Cycler® 480 Real-Time
116 PCR System (Roche, Germany). Because the KASP assays gave the same results as the original
117 GBS SNPs with fewer missing genotype calls, the KASP assays are presented in place of the
118 original GBS SNPs.

119 ***N14 and p779/p780***

120 Parents and progeny from the BRX 44-02 x CIAT 606 mapping population, the *Brachiaria*
121 diversity panel described above, five putatively sexual progeny of the synthetic autotetraploid
122 *Panicum maximum* accession Tift SPM92 (PI 570664; Hanna and Nakagawa 1994), and five
123 accessions each of *C. ciliaris* and *P. maximum* were evaluated with the ASGR-linked SCAR
124 marker N14 and the *ASGR-BBML* specific primers p779/p780. N14 was developed from a RAPD
125 marker (sequence TCGTGCGGGT) discovered by screening 644 random 10-mer
126 oligonucleotide primers (Eurofins MWG Operon LLC, Huntsville, AL) by bulk segregant
127 analysis on parents and progeny of two mapping populations developed from crosses between
128 CIAT BRX 44-02 and the apomictic pollen donors *B. brizantha* CIAT 26646 and CIAT 606
129 (Pedraza Garcia 1995). To convert the RAPD to a SCAR marker, the co-segregating band was
130 excised from *B. brizantha* CIAT 26646 in a low-melting-point agarose gel. The DNA was then
131 isolated using the Wizard PCR Magic kit (Promega Corporation, Madison WI), treated with the
132 Klenow fragment of DNA polymerase, and blunt-end ligated into the PCR-script vector
133 (Stratagene California, La Jolla, CA). *E. coli* DH5 α was transformed with the ligation product,
134 and recombinant clones were selected by X-Gal and IPTG in LB-agar with Ampicillin.
135 Recombinant bacteria were grown overnight and subjected to plasmid minipreps. Double-strand
136 sequencing (Sequenase Kit USB, Affymetrix, Santa Clara CA) was conducted using the dideoxy-

137 chain termination method with T3 and T7 primers. Oligonucleotides were then designed for two
138 of the cloned RAPD amplification products for use as SCAR primers, each with 24 bases
139 (TCGTCGGGTGTTGCGTACTTGTC; TCGTGCGGGTCATGGAGAATTTAT).

140 The N14 primers were used to amplify DNA under the following PCR reaction
141 conditions: 0.3 μ M Primer, 1X GoTaq® Colorless Master Mix (Promega) and 40ng of DNA in an
142 thermocycler programmed with an initial denaturation of 2 min at 95°C, followed by five cycles of
143 touchdown PCR decreasing 1°C per cycle (95°C for 30 s, annealing temperature from 62 to 58°C
144 for 30 s, and 72°C for 60 s), and then 29 cycles of 94°C for 30 s, 58°C for 30 s, and 72°C for 60
145 s, with a final extension step of 72°C for 5 min. Reactions for the p779/p780 primer pair
146 (TATGTCACGACAAGAATATG; TGTAACCATAACTCTCAGCT) (Akiyama *et al.* 2011)
147 were carried out in a final volume of 12 μ l as follows: 40ng of genomic DNA were added to a
148 mix containing 1X GoTaq® Colorless Master Mix (Promega) and 0.5 μ M of each forward and
149 reverse primers. The PCR conditions consisted of an initial denaturation step at 94°C for 5 min
150 followed by 35 cycles of 94°C for 30 secs, 52°C for 30 secs and 72°C for 60 secs, with a final
151 extension step at 72°C for 10 min. Amplified products (12 μ l) for both markers were resolved on
152 1.5% agarose gels stained with SYBR® Safe DNA Gel Stain (ThermoFisher Scientific). Further
153 information on p779/p780 is available on the Integrated Breeding Program diagnostic marker site
154 (<https://www.integratedbreeding.net/298/breeding-services/predictive-markers?marker=58>).

155 ***Linkage Map Construction***

156 Genetic linkage maps of BRX 44-02 and CIAT 606 were constructed separately in JoinMap 4.1
157 following the two-way pseudo-testcross strategy (Van Ooijen 2011). Single-dose allele (SDA)
158 markers that were heterozygous in only BRX 44-02 and homozygous in CIAT 606 were used to
159 construct the maternal map, while SDAs heterozygous in CIAT 606 and homozygous in BRX

160 44-02 were used to build the paternal map. Maps were initially constructed with two datasets: the
161 first dataset included only markers that fit the 1:1 segregation ratio of heterozygote to
162 homozygote progeny expected for SDAs according to a χ^2 test ($P > 0.05$), while the second
163 dataset included distorted markers with segregation ratios less than 2:1. Markers with greater
164 than 20% missing data in the progeny were excluded from both datasets. The CIAT 606 map
165 including the distorted markers had the expected number of linkage groups (n=36), while the
166 map constructed without distorted markers had more linkage groups than expected (n=40),
167 several of which were notably shorter than the other mapped linkage groups (1.2 – 26.3 cM; data
168 not shown). No obvious differences in marker order were observed in the maps created from the
169 two datasets. Therefore, the map including distorted markers is reported in this manuscript
170 (Table S3, Table S4).

171 The threshold linkage logarithm of odds (LOD) score was set to 5.0 to establish initial
172 linkage groups. Marker order was then determined using Monte Carlo maximum likelihood
173 (ML) mapping with default settings (Kyazma). The initial BRX 44-02 map had 38 linkage
174 groups. Subsequently, two pairs of linkage groups that clustered together at LOD 4.0 and 3.0
175 respectively were combined on based on shared synteny with foxtail millet and linkages with
176 double-dose allele (DDA) markers to form a total of 36 linkage groups. A further three
177 previously unlinked markers were added to three poorly saturated linkage groups based on
178 linkage at LOD 3.0 and shared linkages with DDA markers. Charts of genetic linkage maps were
179 drawn using MapChart 2.1 (Voorrips 2002).

180 *Segregation distortion regions*

181 Areas of segregation distortion were identified based on deviation of SDA makers from expected
182 allelic ratios according to the χ^2 test. Log-transformed p-values (-log(p-value)) from χ^2 tests of

183 segregation distortion were plotted against genetic positions for the mapped markers with locally
184 weighted scatterplot smoothing (LOESS) lines using the R package *ggplot2* (Wickham 2009).
185 Regions where the smoothed LOESS curve peaked above LOD = 3 with at least three
186 consecutive markers skewed in the same direction at $P < 0.001$ were classified as distorted
187 according to Li *et al.* (2014).

188 ***Synteny and meiotic associations***

189 The consensus sequences of SDA and DDA tag pairs were first extended using partially
190 assembled 30x WGS sequence data from the diploid *B. ruziziensis* accession CIAT 26162
191 (Unpublished data). Extension was done by aligning the tag reads to the contigs of the partially
192 assembled genome via NovoAlign (www.novocraft.com) then using the contig as the extended
193 tag sequence. The extended tag pair sequences were then queried against the foxtail millet
194 genome (<http://www.phytozome.net/foxtailmillet.php>) (Zhang *et al.* 2012) using the Basic Local
195 Alignment Search Tool (BLAST) with a P -value cutoff of $1e-4$. Markers that aligned to a unique
196 position in the foxtail millet genome were used to assign each linkage group to a chromosome
197 and identify homologues.

198 High resolution molecular karyotyping was used to detect meiotic associations between
199 chromosomal regions with differing degrees of homology and homeology across the paternal
200 CIAT 606 genome (Mason *et al.* 2014). Briefly, each pair of mapped marker alleles was tested
201 for segregation as would be expected for two alleles at a single homologous locus using Fisher's
202 exact test for count data ($P < 0.05$). Deviations from the expected (1:1:1:1) ratio of individuals
203 with both alleles present (1/1), one allele present (0/1 or 1/0), and (0/0) neither allele present
204 were taken as evidence of linkage when an excess of individuals with 0/0 or 1/1 alleles were
205 observed and as evidence for segregation when an excess of individuals with 1/0 or 0/1 scores

206 were found. R version 3.0.0 (The R Project for Statistical Computing) was used to conduct the
207 statistical analysis and generate Heatmap figures following Mason *et al.* (2014) with minor
208 modifications. Chromosome segregation and recombination events in CIAT 606 were also
209 manually inspected by visualization of changes in allele presence or absence along the parental
210 haplotype map in the progeny.

211 Shared linkages with DDA markers were used as further evidence for the identification of
212 homologous linkage groups in the BRX 44-02 map. Markers classified as DDAs segregated at a
213 5:1 ratio of heterozygotes to homozygotes in the F₁ progeny according to a χ^2 test ($P > 0.05$) and
214 less than 20% missing data (Table S3, Table S4). Linkages between DDA and SDA markers
215 from each parental map were assessed in preliminary grouping function of TetraploidMap under
216 simplex-duplex linkages (Hackett *et al.* 2007). Fifty markers from each maternal chromosome
217 (including haplotypes a-d and linked DDAs) were selected based on factors including low levels
218 of missing data, even spacing across the linkage group, and unique positions on the foxtail millet
219 genome for construction of joint maps of *B. ruziziensis* chromosomes 1-9. Marker ordering was
220 conducted with ripple search and simulated annealing settings (Hackett *et al.* 2007).

221 ***Literature cited***

222 Akiyama, Y., S. Goel, J. a Conner, W. W. Hanna, H. Yamada-Akiyama *et al.*, 2011 Evolution of
223 the apomixis transmitting chromosome in Pennisetum. BMC Evol. Biol. 11: 289.

224 Dusi, D. M. A., and M. T. M. Willemse, 1999 Apomixis in Brachiaria decumbens Stapf:
225 gametophytic development and reproductive calendar. Acta. Biol. Cracov. Ser. Bot. 41:
226 151–162.

227 Fisher, S., A. Barry, J. Abreu, B. Minie, J. Nolan *et al.*, 2011 A scalable, fully automated process

228 for construction of sequence-ready human exome targeted capture libraries. *Genome Biol.*
229 12: R1.

230 Hackett, C. A., I. Milne, J. E. Bradshaw, and Z. Luo, 2007 TetraploidMap for Windows: Linkage
231 map construction and QTL mapping in autotetraploid species. *J. Hered.* 98: 727–729.

232 Hanna, W. W., and H. Nakagawa, 1994 Registration of lift SPM92 Sexual Guineagrass
233 Germplasm. *Crop Sci.* 34: 547.

234 Heffelfinger, C., C. A. Fragoso, M. A. Moreno, J. D. Overton, J. P. Mottinger *et al.*, 2014
235 Flexible and scalable genotyping-by-sequencing strategies for population studies. *BMC*
236 *Genomics* 15: 979.

237 Li, X., Y. Wei, A. Acharya, Q. Jiang, J. Kang *et al.*, 2014 A saturated genetic linkage map of
238 autotetraploid alfalfa (*Medicago sativa* L.) developed using genotyping-by-sequencing is
239 highly syntenous with the *Medicago truncatula* genome. *G3 (Bethesda)*. 4: 1971–9.

240 Lu, F., A. E. Lipka, J. Glaubitz, R. Elshire, J. H. Cherney *et al.*, 2013 Switchgrass Genomic
241 Diversity, Ploidy, and Evolution: Novel Insights from a Network-Based SNP Discovery
242 Protocol. *PLoS Genet.* 9: e1003215.

243 Lutts, S., J. Ndikumana, and B. P. Louant, 1994 Male and female sporogenesis and
244 gametogenesis in apomictic *Brachiaria brizantha*, *Brachiaria decumbens* and F1 hybrids
245 with sexual colchicine induced tetraploid *Brachiaria ruziziensis*. *Euphytica* 78: 19–25.

246 Mason, A. S., J. Batley, P. E. Bayer, A. Hayward, W. A. Cowling *et al.*, 2014 High-resolution
247 molecular karyotyping uncovers pairing between ancestrally related *Brassica* chromosomes.
248 *New Phytol.* 202: 964–974.

- 249 Van Ooijen, J. W., 2011 Multipoint maximum likelihood mapping in a full-sib family of an
250 outbreeding species. *Genet. Res.* 93: 343–349.
- 251 Oram, R. N., 1990 *Register of Australian herbage plant cultivars*. Australian Herbage Plant
252 Registration Authority, Division of Plant Industry, CSIRO, East Melbourne, Australia.
- 253 Pedraza Garcia, F. P., 1995 *Hacia la localización del gen de apomixis en Brachiaria usando*
254 *marcadores moleculares RAPD [thesis]*. Universidad Nacional de Colombia, Palmira, Valle
255 del Cauca.
- 256 Risterucci, A. M., L. Grivet, J. A. K. N’Goran, I. Pieretti, M. H. Flament *et al.*, 2000 A high-
257 density linkage map of *Theobroma cacao* L. *Theor. Appl. Genet.* 101: 948–955.
- 258 Shure, M., S. Wessler, and N. Fedoroff, 1983 Molecular identification and isolation of the Waxy
259 locus in maize. *Cell* 35: 225–233.
- 260 Swenne, A., B. Louant, and M. Dujardin, 1981 Induction par la colchicine de formes
261 autotétraploïdes chez *Brachiaria ruziziensis* Germain et Evrard (Graminée). *Agron. Trop.*
262 36: 134–141.
- 263 Valle, C. B., Y. H. Savidan, and L. Jank, 1989 Apomixis and sexuality in *Brachiaria decumbens*
264 Stapf, pp. 407–408 in *XVI International Grassland Congress*, INRA, Nice, France.
- 265 Voorrips, R. E., 2002 MapChart: software for the graphical presentation of linkage maps and
266 QTLs. *J. Hered.* 93: 77–78.
- 267 Wickham, H., 2009 *ggplot2: Elegant Graphics for Data Analysis*. Springer-Verlag, New York.
- 268 Zhang, G., X. Liu, Z. Quan, S. Cheng, X. Xu *et al.*, 2012 Genome sequence of foxtail millet
269 (*Setaria italica*) provides insights into grass evolution and biofuel potential. *Nat. Biotechnol.*

270 30: 549–54.

271